

University of Nebraska - Lincoln

DigitalCommons@University of Nebraska - Lincoln

Civil and Environmental Engineering Theses,
Dissertations, and Student Research

Civil and Environmental Engineering

Spring 4-27-2022

Performance of Concrete with Different Cement Finenesses and Nano-activators

Brandon Faltin

University of Nebraska-Lincoln, bfaltin2@huskers.unl.edu

Follow this and additional works at: <https://digitalcommons.unl.edu/civilengdiss>



Part of the [Civil Engineering Commons](#), and the [Other Civil and Environmental Engineering Commons](#)

Faltin, Brandon, "Performance of Concrete with Different Cement Finenesses and Nano-activators" (2022). *Civil and Environmental Engineering Theses, Dissertations, and Student Research*. 178. <https://digitalcommons.unl.edu/civilengdiss/178>

This Article is brought to you for free and open access by the Civil and Environmental Engineering at DigitalCommons@University of Nebraska - Lincoln. It has been accepted for inclusion in Civil and Environmental Engineering Theses, Dissertations, and Student Research by an authorized administrator of DigitalCommons@University of Nebraska - Lincoln.

PERFORMANCE OF CONCRETE WITH DIFFERENT CEMENT FINENESSES AND
NANO-ACTIVATORS

by

Brandon Faltin

A THESIS

Presented to the Faculty of
The Graduate College at the University of Nebraska
In Partial Fulfillment of Requirements
For the Degree of Master of Science

Major: Civil Engineering

Under the Supervision of Professor Jiong Hu

Lincoln, Nebraska

May 2022

PERFORMANCE OF CONCRETE WITH DIFFERENT CEMENT FINENESSES AND NANO-ACTIVATORS

Brandon Faltin, M.S.

University of Nebraska, 2022

Advisor: Jiong Hu

The excessive shrinkage in modern concrete is the result of the construction industry in its quest to complete the job as soon as possible. In order to accomplish this, the fineness of cement was increased significantly in recent decades for a faster rate of strength gain. To combat the cement fineness and reverse the trend of shrinkage, the usage of coarse cements and nanoparticles should be strongly considered. The coarse cement is used to reduce the shrinkage of concrete, while the nanoparticle increases the early strength, alleviating the original concerns of reduced early strength when using coarse cement.

Work in this study provides enough evidence toward coarse cement and nanoparticle use being extremely beneficial to concrete. In particular, the coarse cement reduces the shrinkage, while the incorporation of nanoparticles not only improves the initial strength gain, but also further decreases the shrinkage. At the age of seven days, the mixtures using coarse cement with nanoparticles show a compressive strength greater than the Type I/II mixtures used as reference. Regarding shrinkage, the use of nanoparticles in mixtures with coarse cement outperformed the coarse cement by itself. Thus, the use of nanoparticles as an activator in coarse cement concrete is considered a viable option for applications where low shrinkage and long-term durability are desirable.

ACKNOWLEDGEMENTS

I would like to first thank Dr. Jiong Hu, for his support. At times, I could forget my direction in this research, and he was always able to help me see the path forward. Despite all the troubles in equipment I brought forward, he remained a positive force for me.

I would like to express my appreciation and gratitude to my thesis committee members, Dr. Congrui Grace Jin, and Dr. Marcus Maguire for agreeing to review and provide feedback on this thesis.

Furthermore, I would like to thank the Materials and Geotechnical research group of the University of Nebraska, both current and former members, Dr. Miras Mamirov, Dr. Flavia Mendonca, Mr. Termilan Barissov, Mr. Arafat Alam, Ms. Akbota Aitbayeva, Mr. Andrew Ruder, Mr. Jose Cortes, and Mr. Rodrigo Quintero for all their assistance from knowledge of concrete to physical assistance in the laboratory.

TABLE OF CONTENTS

TABLE OF CONTENTS.....	ii
TABLE OF FIGURES.....	iv
TABLE OF TABLES	v
CHAPTER 1. INTRODUCTION.....	1
1.1. Background	1
1.2. Research Significance	3
1.3. Objectives.....	3
1.4. Thesis Organization.....	4
CHAPTER 2. LITERATURE REVIEW	5
2.1. Introduction	5
2.2. Roman Concrete.....	5
2.3. Impact of Cement Fineness on Concrete Performance	8
2.4. Impact of Nanomaterials on Concrete Performance	10
2.4.1. Types of Nanomaterials.....	10
2.4.2. Production of Nanomaterials.....	11
2.4.3. Influence of Nanomaterials on Hydration	12
2.4.4. Influence of Nanomaterials on Fresh Concrete Performance.....	12
2.4.5. Influence of Nanomaterials on Hardened Concrete Performance	13
CHAPTER 3. MATERIALS AND TEST METHODS.....	16
3.1. Materials.....	16
3.1.1. Cement.....	16
3.1.2. Nanomaterials.....	16
3.1.3. Aggregate.....	17
3.2 Mixture Proportions	17
3.3. Mortar Mixing Procedure.....	19
3.4. Specimen Size and Preparation.....	21
3.5. Fresh and Early Age Mortar Tests	23
3.5.1 Flow Table Test.....	23
3.5.2. Unit Weight Test	24
3.5.3. Heat of Hydration Test	24
3.5.4. Autogenous Shrinkage.....	25

3.6. Hardened Mortar Tests.....	29
3.6.1. Compressive Strength.....	29
3.6.2. Drying Shrinkage.....	30
3.6.3. Microstructure Analysis	31
CHAPTER 4. RESULTS AND DISCUSSION.....	33
4.1. Workability.....	33
4.2. Heat of Hydration.....	36
4.3. Compressive Strength	41
4.4. Microstructure Analysis	44
4.5. Shrinkage.....	47
CHAPTER 5. CONCLUSION AND RECOMMENDATIONS	55
5.1. Conclusions	55
5.2. Recommendations for Future Work.....	56
REFERENCE LIST	58

TABLE OF FIGURES

Figure 1.1. Synergy of coarse cement and nano-activator.....	2
Figure 2.1. Location of Campi Flegrei, Italy	6
Figure 2.2. Enhanced view of Campi Flegrei	7
Figure 2.3. Specific surface area of particles with different fineness	11
Figure 3.1. Mixer used in this study	20
Figure 3.2. Higher shear blender and cylinder used to pre-blend nanomaterial	21
Figure 3.3. Flow Table Test Apparatus	23
Figure 3.4. Isothermal Calorimeter	25
Figure 3.5. Support Frame for Casting Autogenous Shrinkage Samples	26
Figure 3.6. Autogenous shrinkage test apparatus and samples.....	28
Figure 3.7. Compressive strength apparatus	29
Figure 3.8. Drying shrinkage testing apparatus	30
Figure 3.9. SEM Samples before and after resin casting.....	31
Figure 3.10. Diamond tipped saw	32
Figure 4.1. Flow table test results with changing w/c	34
Figure 4.2. Flow table test results of changing dosage of nanoparticles	35
Figure 4.3. Heat of hydration curves	37
Figure 4.4. Compressive strength results from changing w/c ratio	42
Figure 4.5. Compressive strength of changing dosage and fineness	43
Figure 4.6. SEM images of samples at 1 day of hydration	45
Figure 4.7. SEM images of samples at 7 days of hydration	46
Figure 4.8. Autogenous shrinkage results.....	48
Figure 4.9. Long- and mid-term drying shrinkage.....	52
Figure 4.10. Combined shrinkage results	54

TABLE OF TABLES

Table 3.1. Chemical Composition of Cement and Nanomaterial	17
Table 3.2. Mixture Proportions.....	18
Table 4.1. Heat produced during isothermal calorimeter testing.....	40

CHAPTER 1. INTRODUCTION

1.1. Background

The ever-increasing demands of the construction force the hands of the cement industry to produce high early strength cements. Simultaneously, shrinkage related deteriorations increased in quantity. Denver faced such a problem during the 1990's, where several bridges needed to be replaced in order to meet traffic demands as well as the construction of the new Denver International Airport. The original bridges being replaced did not crack during the 50-year service life and were of a low early strength cement. Testing of samples prepared during the replacement bridge construction showed high strength, 5600 psi at seven days. At the airport, the samples prepared were also of high strength at between 4520 and 5380 psi at the age of seven days. The deterioration to the bridges were quite significant, with cracking of the concrete occurring before completion for several bridges and a high volume of cracking during the first three months of service. One of the bridges needed construction joint spacing reduced from 9 ft. to 4 ft. and placed at night to reduce the risk of cracking; yet the concrete still cracked. At the airport, over 10,000 panels showed enough cracking to be a concern for aircraft. There is a common underlying factor in each of these projects, which is the concrete cracked due to high shrinkage (Burrows 2007).

The high shrinkage should be a higher concern as the early cracking allows for other deteriorating agents to attack the concrete sooner. However, there does not need to be early shrinkage concerns. Using a coarse ground cement, not unlike what had been used in the early to mid-1900's, could be the potential solution. The concern with using a

coarse ground cement is its low early strength, which however, can be mitigated by adding a nanoparticle to the concrete mixture. Nanoparticles serve as a nano-activator for the cement through the “nucleus effect” and additionally add a smaller size of particles to increase particle packing through the “filler effect” (Siddique & Klaus 2009). Through the “nucleus effect”, the cement particles have increased points of contact for hydration, allowing for more rapid strength gain (Gleize et al. 2007). Further, the “filler effect” reduces the pore sizes in the cement paste which can provide additional benefits to the cementitious matrix (Sabir et al. 2001). The nanoparticles are chemically made from silica dioxide or aluminum dioxide, allowing for pozzolanic reaction providing even further benefit to the cementitious matrix. Thus, by adding nanoparticles to concrete using a coarse ground cement, the concern of low early strength can be alleviated.

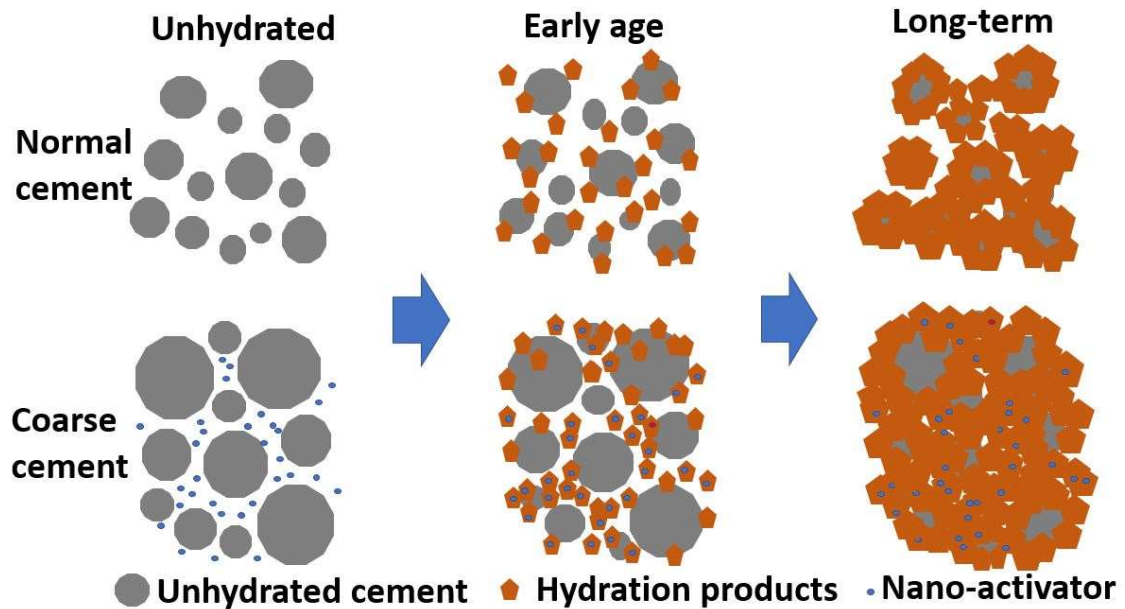


Figure 1.1. Synergy of coarse cement and nano-activator

1.2. Research Significance

Understanding the connection between the autogenous and drying shrinkage is of high importance. Reducing the early shrinkage through measuring autogenous shrinkage and early drying shrinkage is the key idea in using the coarse cement, but if adding nanoparticles increases long term shrinkage found in drying shrinkage, the solution does not work. Thus, necessitating measuring both of these types of shrinkage and combining the data to form a clear picture. Additionally, the rate of strength gain is necessary in order to be a viable alternative to current concrete. Further, a known effect of nanoparticles is a decrease in workability and as such, the flow table test is performed (Sanchez & Sobolev 2010). Finally, the heat of hydration test is performed simultaneously with the autogenous shrinkage test in order provide necessary data discussed later on. With few studies focusing on the autogenous shrinkage of mortar with nanoparticles, this study emphasizes the effect nanoparticles have on the early age properties of mortar. Additionally, this study points to how a change in evaluating shrinkage data is necessary.

1.3. Objectives

The overall objective of this study was to determine the feasibility of using a coarse ground cement, first by itself, then in combination with nanomaterials to reduce the shrinkage of concrete used today. Firstly, nanomaterials were identified as being directly beneficial to reducing the shrinkage of concrete. Secondly, a cement of similar composition was acquired but with a lower Blaine fineness number than current Type I/II. From this, a plan to identify the effects of using the nanomaterials through Heat of Hydration, Flow Table, Unit Weight, compressive strength, autogenous shrinkage, and

drying shrinkage. Furthermore, the use of a Scanning Electron Microscope (SEM) was used to visually confirm the effects of the nanomaterial on the cementitious matrix.

1.4. Thesis Organization

This report is divided into five chapters, beginning with the Introduction. Following which, Chapter 2 provides a detailed review by covering the topics of Roman Concrete, Cement Fineness and its impacts, and finally the Impact of Nanoparticle usage. Chapter 3 presents the materials in this report as well as the methods applied. Penultimately, Chapter 4 analyzes the results and provides a commentary for discussion. Finally, Chapter 5 concludes the report by summarizing the findings and presenting recommendations for future work.

CHAPTER 2. LITERATURE REVIEW

2.1. Introduction

Concrete today is different than it was 50 years ago, but it is not because of moving to a different internal material, rather, it is largely due to a change within cement. Over the last 50 years, a move toward higher Blaine fineness cement, driven by the pace of construction, has led to earlier distress in concrete. Such early distress and deterioration should be considered unacceptable yet is allowed to remain. The solution is in the past. Using a coarse ground cement, reminiscent of what was used prior to the 1970's and synergizing it with a nano-activator in order to compensate for low early age strength. In this, the early strength of modern concrete is preserved and the low deterioration of 1970's returns.

2.2. Roman Concrete

Concrete used today is significantly different than what was used thousands of years ago by Roman architects Herod and Vitruvius. Today, the use of volcanic ash and lime has been replaced by cement and cementitious materials, and pumice and tuff by local aggregates. However, the concept of concrete remains the same; use a binder and mix it with aggregates in order to create a material capable of withstanding load.

Roman concrete is famous for its achievements which are still standing today, such as the Pantheon, aqueducts, and piers in harbors around the Mediterranean Sea. Despite 2,000 years of weathering, saline conditions, earthquakes, and war, these structures are in remarkably good condition. However, when looking at these amazing time capsules, it is important to note the survivor bias. The only structures seen today

from the time of the Romans is the best of the best (Malisch 2017). What cannot be seen, are the structures which failed under earthquakes, landslides, collapses, floods, and lack of maintenance (Jackson et al. 2014).

Comparing to modern concrete, Roman concrete lacks reinforcing steel to resist tensile forces. The lack of steel rebar corrosion to deteriorate Roman concrete removes a significant source of modern concrete deterioration. This now reduces the detriments of Roman concrete only to external forces.



Figure 2.1. Location of Campi Flegrei, Italy

Another factor in the longevity of Roman concrete is the mild climate of the Mediterranean Sea. The distinct lack of lengthy cold weather and snowfall, in combination with no de-icing salts applied, reduce further chances of accelerated deterioration due to climatic and human forces. Removing these forces as sources of degradation increases the longevity of Roman concrete (Malisch 2017).

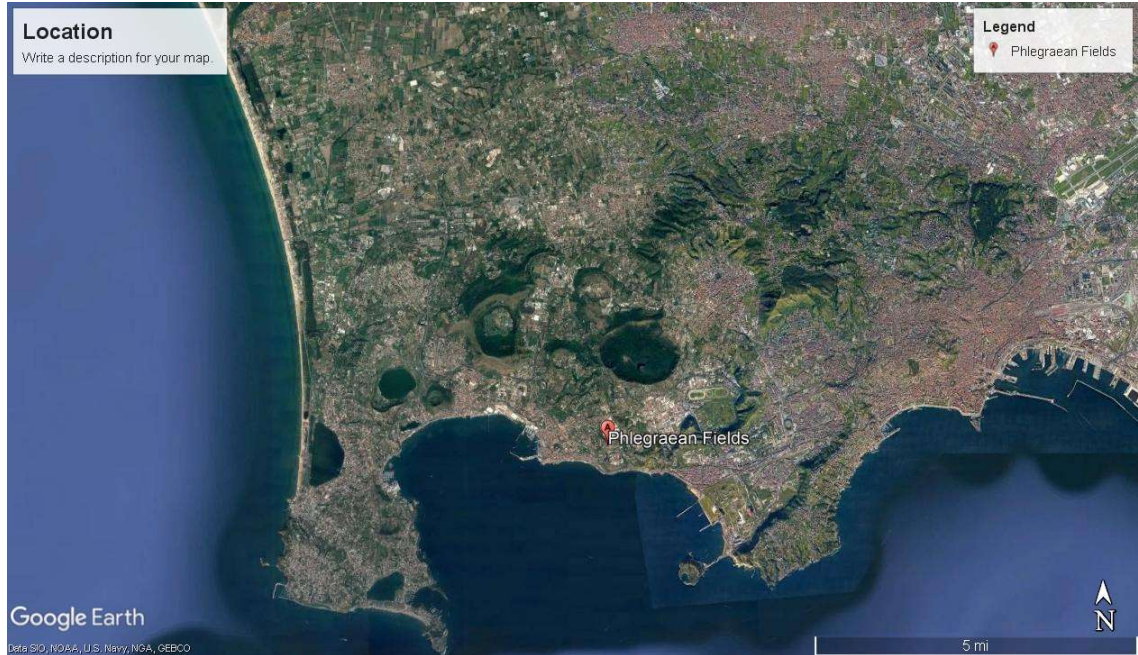


Figure 2.2. Enhanced view of Campi Flegrei

In searching for the reason why Roman concrete lasted so long, it is also important to look at the materials used in the concrete. Specifically, volcanic rock and ash are of interest. The famous architect Vitruvius refers directly to a specific source of volcanic ash from the region of the volcano Campi Flegrei, near the modern town of Pozzuoli, Italy (Jackson et al. 2014). Volcanic ash from this area contains a larger amount of Aluminum than usual at the cost of the Silica content. During the hydration process, Aluminum forms the crystal Al-Tobermorite and the fiber Stratlingite, increasing the bond strength of the cementitious matrix and bridging cracks respectively. This Calcium Aluminum Silica Hydrate can be shortened to C-A-S-H (Jackson et al. 2013).

Volcanic ash from Pozzuoli is where the term pozzolanic comes from, a reference to Roman concrete. Another reference to the Romans comes in the form of the cement fineness. Low cement fineness is very similar to the slaked lime created from mortar and pestle by the Romans. Roman concrete did not gain strength at an early age due to the

lower cement fineness. The reason behind this is the lower demand for the material to be in use immediately. Low cement fineness and low demand for high early strength were retained through the 1900's and up until relatively recently when external forces compelled changes to cement fineness.

2.3. Impact of Cement Fineness on Concrete Performance

Over the course of the last 50 years, construction demands have forced the hand of the cement industry to provide higher early strength cement. In order to achieve the early strength, the previous standards, recommendations, and practices were abandoned, and the Blaine fineness of cement was drastically increased. In coordination with increasing fineness, tricalcium silicate (C_3S) and tricalcium aluminate (C_3A) increased as well to achieve higher strength (Burrows 2012).

The purpose of Type II cement originally, was to reduce cracking of concrete. In order to do so, a limit of 58% was placed on the combined content of C_3S and C_3A in cement considered Type II (Burrows 2007). Returning to the construction in Denver as mentioned earlier, the cement used in the concrete was specified as Type II. In a study of the Type II cement used in Colorado around this same time (1996- 2002), the combined C_3S and C_3A content was 72%. The cement was out of specifications and needed to be reclassified as Type I/II.

Again, sourcing from Burrows (2007), from a study in 1994 with a wider range covering Type II cements in the United States, 33 of the 147 cements met the 58% combined C_3S and C_3A content specifications for Type II cement. In addition, a 1954 study of Type II cements found concrete made with these cements had a 3-day

compressive strength of less than 3,000 psi. In 1999, just 45 years later, a study of the same Type II cements found 89% of these cements made concrete above 3,000 psi at 3-day compressive strength. Under an American Concrete Institute (ACI) task force in 1979, recommendations were made to reclassify all Type II cements with resulting concrete compressive strengths above 3,000 psi to be Type III cement. The recommendation from the ACI task force was not accepted. Returning to Denver again, the 7-day compressive strength samples taken reached between 4520 psi and 5380 psi with a high of 5600 psi. Such an increase in compressive strength combined with the knowledge of the combined C_3S and C_3A content of 72% reaches one conclusion: High C_3S and C_3A and high Blaine fineness, resulting in high early compressive strengths are detrimental to the longevity of concrete (Burrows 2007).

From Burrows (2007), prior to the ACI task force of 1979, Bryant Mathers visited Europe in 1965 and noticed European cement was limited on strength and fineness. Mathers' recommendation to the American Society of Testing and Materials (ASTM) to limit the early strength and fineness of the cements was also rejected. It is important to note, at this point in time, the cement being used produced concrete with minimal cracking.

Adam Neville in 1987 is quoted as saying, "Anything that increases the rate of hydration of cement, is detrimental to the durability of concrete" (Burrows 2007). Hydration, being the reaction of cement and water, increases in reaction rate as fineness of cement and C_3S/ C_3A content increases. Increasing the speed at which hydration reacts, directly corresponds to the internal stresses developed by the concrete, which resolves the stresses by shrinking. Coarse ground cement has lower shrinkage as a result

of lower internal stresses (Bentz et al. 2006). When Europeans look for concrete that will not crack, it looks toward a cement like Type 32.5 which has a limited fineness and upper limit on its 7-day compressive strength (Burrows 2012).

Limiting the C_3S and C_3A content as well as fineness outside the U.S. has performed extremely well. In Sweden, the fineness is limited and the C_3A content is controlled to 0%. Montreal also limits its C_3A content specifically to 5% but would like to reduce this further. Additionally, the Three Gorges Dam in China limited the C_3S and C_3A content in order to control cracking on the behemoth structure (Burrows 2007).

Concerns about the fineness of the cement are interconnected through hydration. While compressive strength and shrinkage have been mentioned earlier, left out is the thermal increase associated with high fineness. There is a direct isothermal increase in cement with high fineness over a low fineness (Bentz et al. 2006). In order to combat the high heat produced, multiple methods such as fly ash, night placement, and ice are used (Schindler & McCullough 2002).

2.4. Impact of Nanomaterials on Concrete Performance

2.4.1. Types of Nanomaterials

In a low cement concrete, the largest concern is the low early strength of the concrete. In order to improve the low early strength, supplemental materials must be included into the concrete mixture. This is where nanomaterials come into play.

Nanomaterials include calcined clays and pure materials which when included into concrete, enhance properties related to the cementitious matrix. Of particular note are

nanosilica and metakaolin, with others such as nanotitanium and nano-iron being options for use but not considered in this study.

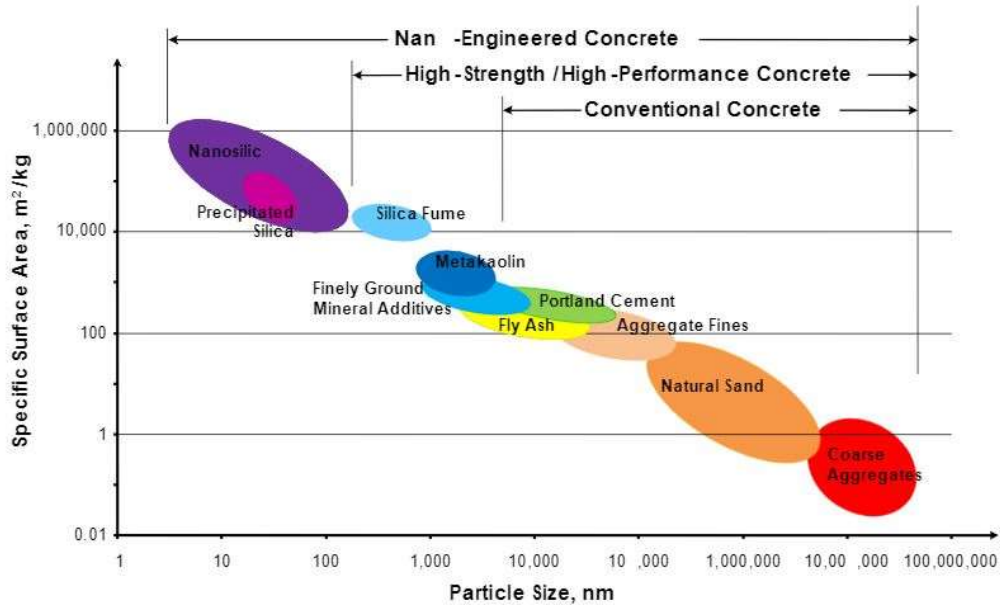


Figure 2.3. Specific surface area of particles with different fineness

Adopted from (Sobolev et al. 2006)

2.4.2. Production of Nanomaterials

Nanomaterial production comes from the Sol-gel method as well as mining, depending on if the material is pure, such as nanosilica or a natural clay such as metakaolin. Metakaolin, or similar clays, must be mined before being placed in a kiln to a temperature between 700° and 900° C (Glavind 2009). The sol-gel method requires the use of stoichiometry and chemistry to produce a soluble of the desired chemical. After which, the soluble is dried out to produce a pure product such as TiO₂ and SiO₂ in the nano-form (Akpan & Hameed 2010).

2.4.3. Influence of Nanomaterials on Hydration

Nanomaterials change cement hydration in a large way. In large part, this comes from the “Nucleus Effect” associated with the use of nanoparticles. The Nucleus Effect is the seeding of additional points of cement hydration through the use of very fine particles (Sabir et al. 2001). Additionally, the hydration is impacted by the “Pozzolanic Effect” where known pozzolanic materials react with the Calcium Hydroxide (C-H) in order to produce Calcium Silica Hydrate (C-S-H) (Sanchez & Sobolev 2010). Nanosilica (Birgisson et al. 2012) and metakaolin (Siddique & Klaus 2009) both introduce additional silica while only metakaolin introduces aluminum into the hydration process. Both of these elements react pozzolanically, reducing the calcium ions, to produce additional C-S-H gel in the cementitious matrix (Gaitero et al. 2010).

When looking at a normal cementitious matrix, C-S-H gel makes up approximately 50-70% of the matrix (Shah et al. 2008). This number is refined further to about 60% by volume by Raki et al. (2010). The inclusion of nanomaterials increases this due to the pozzolanic reaction consuming C-H. Looking at nanosilica specifically, the silicate chains in C-S-H increased in length due to the increased silica present in the matrix (Glenn 2013). In addition, Gaitero (2010) noticed an increase in high-density gel and a decrease in low-density gel.

2.4.4. Influence of Nanomaterials on Fresh Concrete Performance

Including either of metakaolin or nanosilica in concrete is known to reduce the workability of the mixture due to an increase surface area. Increasing the dosage above 5% caused further reduction to workability and flow. In order to maintain flow from the reference mix design, the mixture with nanomaterials experience an increased water

demand (Tobón et al. 2010). Srinivas (2014) attributes the change in workability to a higher packing density when nanoparticles are added. Further work by Sobolev (2006) with nanosilica also found a similar reduction in the flow and workability. For metakaolin, Sabir et al. (2001) and Siddique and Klaus (2009) both found a similar reduction in the flow table results. Sabir et al. (2001) specifically mentioned the reduction of high-range water reducer needed to retain workability in comparison to silica fume, a reduction of around 25-35%. Furthermore, the reduction of workability by the addition of metakaolin is attributed to the filler effect by Siddique and Klaus (2009).

When looking at metakaolin specifically, Gleize et al. (2007) notes the autogenous shrinkage increases when using metakaolin. This is attributed to the “Nucleus Effect” mentioned previously (Sabir et al. 2001). Wang et al. (2020) concludes a similar point when working with nanosilica. The accelerated hydration via the “Nucleation Effect” increases the tensile stresses generated by the concrete mixture (Almohammad & Behfarnia 2020).

2.4.5. Influence of Nanomaterials on Hardened Concrete Performance

Through the use of nanomaterials, the cementitious matrix changes and as a result, the hardened mortar properties change. As part of this, there is a strength increase. As mentioned before, the “Filler Effect” in combines with the “Nucleus Effect” in order to create a stronger cementitious matrix. Chemically, the nanosilica and metakaolin introduce additional free silica into the matrix, allowing calcium ions to hydrate with the silica to produce more of the Calcium Silica Hydrate (C-S-H) (Birgisson et al. 2012). The resulting compressive strengths of mixes with nanosilica due to this strengthened matrix were higher than mixtures with silica fume (Srinivas 2014). When looking at the use of

metakaolin, the increased matrix strength provided not only additional compressive strength, but tensile and bending strength as well at high dosages (Siddique & Klaus 2009).

Both metakaolin and nanosilica are shown to be capable of reducing the drying shrinkage. This decrease comes from the refined pore structure due to the filler effect and pozzolanic effect. Metakaolin reduces the drying shrinkage by around 5% (Brooks & Johari 2001). With this reduced shrinkage is a long-term durability increase (Gruber et al. 2001). Nanosilica is similar in that it decreases the drying shrinkage and increases the long-term durability (Raki et al. 2010). It should be noted here, the decrease in drying shrinkage does coincide with the dosage. As dosage is decreased, so do the benefits (Almohammad & Behfarnia 2020).

While not explored in this study, metakaolin does provide additional benefits to concrete. First being the reduction of Alkali-Silica Reaction (ASR) occurring (Courard et al. 2003). At a large dosage of 10%, metakaolin showed a high resistance to ASR, further benefitting the long-term durability of the concrete (Gruber et al. 2001). Siddique and Klaus (2009) present 10-15% dosages are enough to control ASR deterioration entirely rather than slow it down. Additionally, metakaolin reduces the amount of creep in concrete. Brooks and Johari (2001) associate the reduction in creep with the reduction in free water and refined pore structure.

When specifically mentioning nano-titanium, the photocatalytic effect is one extremely useful benefit. Capable of removing pollutants from the air, the photocatalytic effect combines ultraviolet radiation from sunlight to induce a change in the electrons of the titanium dioxide atom. This change in electrons promotes absorption of pollutants

such as nitrogen monoxide and releases substances such as water. Additionally, nano-titanium was used to improve compressive strength, however the results above a 3% dosage resulted in strength reduction. Due to the lack of pozzolanic reaction taking place, nanosilica is more beneficial when comparing the cementitious matrix of these two supplemental materials (Silvestre et al. 2016).

CHAPTER 3. MATERIALS AND TEST METHODS

This chapter describes materials used within this study, along with the mixing procedure and tests to be performed.

3.1. Materials

3.1.1. Cement

The focus within this study is on the cement fineness, and as such uses a Type I/II cement, a coarse ground cement of similar composition, and a Type III cement in some cases, with the compositions of these cements located in Table 3.1 (ASTM C150). The Type I/II cement used as a reference has a Blaine Fineness of 417 m²/kg, and the coarse ground cement has a reduced fineness of 312 m²/kg.

3.1.2. Nanomaterials

Along with the cement, the use of nanomaterials is included in the mixture designs and the properties of the metakaolin and nanosilica are also found in **Error! Reference source not found.** Of note, the metakaolin has a significantly lower Blaine fineness (1,000- 5,000 m²/kg) compared to the nanosilica (20,000-50,000 m²/kg).

Table 3.1. Chemical Composition of Cement and Nanomaterial

	Type I/II Cement	Coarse Cement	Type III Cement	Nanosilica	Metakaolin
C ₃ S %	61	66	58	-	-
C ₂ S %	11	9	14	-	-
C ₃ A %	6	7	7	-	-
C ₄ AF %	9	11	9	-	-
SiO ₂ %	20.2	20.4	20.2	99.7	55.01
Al ₂ O ₃ %	4.3	4.9	4.5	-	40.94
Fe ₂ O ₃ %	2.9	3.6	3.0	-	0.55
CaO %	64	65.3	63.3	-	0.14
MgO %	1.8	0.7	2.0	-	0.34
SO ₃ %	2.8	2.2	4.1	<0.03	-
Na ₂ O %	0.15	0.26	0.19	<0.05	0.09
K ₂ O %	0.56	0.4	0.56	-	0.6
TiO ₂ %	-	-	-	-	0.55

3.1.3. Aggregate

For the remaining materials, the use of river sand from the Platte River in Nebraska conforming to ASTM C37 (ASTM C37) gradation requirement and tap water-free of oils and chemical detriments- are included in the mortar mixes meeting ASTM C305 (ASTM C305). The river sand's properties are an oven-dry specific gravity of 2.60, saturated surface dry specific gravity of 2.62, apparent relative density of 2.66, and an absorption of 0.9% (ASTM C128).

3.2 Mixture Proportions

Mortar batching was based on the recommended mortar ratios for w/c of 0.485 and s/c 2.75 from ASTM C109/109M (ASTM C109). To explore the effects of nanomaterials, the nanomaterials are used as an additive in the mixture, ensuring the w/c ratio remains the same. Because the goal of this research was to study the impact of usage of nanoparticles in order for large scale applications to be feasible, only lower dosages of

the nanomaterials were considered despite literature presenting results with higher dosages of 10% (Gruber et al. 2001), 10-15% (Siddique & Klaus 2009), 15% (Courard et al. 2003), and 10% (Sanchez & Sobolev 2010).

From Table 3.2, the mixture proportions are shown with the relevant cement and nanomaterial. Different w/c ratios are considered to test the decrease of flow table results and workability. The dosage of nanomaterials changes in order to reveal the results of lower dosages.

Table 3.2. Mixture Proportions

Mix ID	Cement Type	Nanoparticle Type	Contents (PCY)			
			Cement	Nano-particle	Fine Aggregate	Water
NC-0.45	Type I/II	-	550	0	1513	248
CC-0.45	Coarse	-	550	0	1513	248
NSN-0.45 3%	Type I/II	Nanosilica	546	16	1503	246
MKN-0.45 3%	Type I/II	Metakaolin	546	16	1503	246
NC-0.485	Type I/II	-	540	0	1484	262
CC-0.485	Coarse	-	540	0	1484	262
NSN-0.485 3%	Type I/II	Nanosilica	536	16	1475	260
MKN-0.485 3%	Type I/II	Metakaolin	536	16	1475	260
NC-0.52	Type I/II	-	530	0	1457	275
CC-0.52	Coarse	-	530	0	1457	275
NSN-0.52 3%	Type I/II	Nanosilica	526	16	1447	274
MKN-0.52 3%	Type I/II	Metakaolin	526	16	1447	274
NSN-0.485 1%	Type I/II	Nanosilica	539	9	1481	261
MKN-0.485 1%	Type I/II	Metakaolin	539	9	1481	261
NSN-0.485 5%	Type I/II	Nanosilica	534	27	1468	259
MKN-0.485 5%	Type I/II	Metakaolin	534	27	1468	259
NSC-0.485 3%	Coarse	Nanosilica	536	16	1475	260
MKC-0.485 3%	Coarse	Metakaolin	536	16	1475	260
NS3-0.485 3%	Type III	Metakaolin	536	16	1475	260
MK3-0.485 3%	Type III	Metakaolin	536	16	1475	260

3.3. Mortar Mixing Procedure

Mortar was mixed according to the procedure in ASTM C305 with a small batch size of 0.0014 m^3 (0.065 ft^3) (ASTM C305) with the mixer being used found in Figure 3.1. Water is placed in the bowl, paddle attached, and cement added before starting the mixer. After adding the cement, mix at low speed for 30 seconds before adding the fine aggregate over the course of the next 30 seconds while continuing to mix. Increase the speed to medium for 30 seconds before pausing the mixer to scrape the sides of the bowl and paddle. Cover the mixer with a plastic tarp to prevent moisture loss during this 90 second period. Restart the mixer for 60 seconds on medium speed to complete the mixing. When the mixture design calls for a nanomaterial to be added, the total amount of water is placed in the high shear blender seen in Figure 3.2 prior to the above mixing procedure, nanomaterial is added to the blender, then the blender is turned on for 60 seconds. This blended water and nanomaterial are to be placed in the mixing bowl and the procedure begins.



Figure 3.1. Mixer used in this study



Figure 3.2. Higher shear blender and cylinder used to pre-blend nanomaterial

3.4. Specimen Size and Preparation

After completion of the mixing procedure, testing of the fresh samples and casting begins. To provide a rough timeline, ASTM C1437 Flow Table test is performed immediately after completing mixing (ASTM C1437). Following this, the Fresh Unit

Weight (ASTM C138/138M) and Heat of Hydration tests are performed (ASTM C1702). Finally, compressive strength cubes (ASTM C109/109M), shrinkage bars (ASTM C596), and autogenous shrinkage tubes (ASTM C1698) are cast. The entire process from water to cement contact to finish should take approximately 22 to 25 minutes.

In the initial set of mixes, nine 50 mm x 50 mm x 50 mm (2" x 2" x 2") cubes are set aside and oiled before mixing along with one 50 mm x 100mm (2" x 4") cylinder to be used in the Fresh Unit Weight test. After completion of the mixing, the cylinder is filled first for unit weight. Following this, the cubes are consolidated and finished according to ASTM C109 (ASTM C109/109M). The cubes are left to cure under a damp towel and plastic for 24 hours before demolding and placing in a curing room of 100% humidity at 23°C.

Secondary mixes retain the same volume; however, it changes the samples casted and tested. Three 50mm (2") cubes are used instead of nine with the volume instead being used toward four 25 mm x 25 mm x 250 mm (1" x 1" x 11.25") shrinkage bars and one corrugated tube 420 mm x 29 mm (16.5" x 1.2"). The shrinkage bars conform to ASTM C596 (ASTM C596), and the corrugated tube is in accordance with ASTM C1698 (ASTM C1698). For the shrinkage bars, hand consolidation is used with 12 tampers per layer in two layers per bar. In preparing the corrugated tube, one end is plugged with a cap covered in vacuum grease while leaving the second end open. The corrugated tube is filled with the aid of a vibration table, PVC casting support tube, funnel, and human assistant. Vibration is used for between 1 and 2 minutes depending on the stiffness of the mix. After filling the corrugated tube, the other plug is covered in vacuum grease and used to seal the tube.

3.5. Fresh and Early Age Mortar Tests

3.5.1 Flow Table Test

For Fresh mortar, ASTM C1437, Flow Table Test, found in **Figure 3.3**, is the first test performed after mixing is completed (ASTM C1437). In accordance with this test, the conical mold is filled with the mortar and consolidated. After which, the mold is removed, and the assembly is dropped a total of 25 times in 15 seconds. The resulting diameter is measured four times along the indicated lines on the table surface. To describe the flow of the test, the result is represented as an increase of the original cone base.



Figure 3.3. Flow Table Test Apparatus

3.5.2. Unit Weight Test

The final test for fresh mortar is the unit weight test using the 50 mm x 100 mm cylinder as mentioned before. After zeroing the scale with the cylinder on it, two layers of mortar are cast with 25 hand tampers per layer. While nanomaterial does not add a significant amount of mass to the mixture, this test does ensure the samples are uniform before casting of hardened mortar properties. The fresh mortar tests should be completed around the 12-minute mark after starting the mixing process.

3.5.3. Heat of Hydration Test

Following the Flow Table Test is the Heat of Hydration Test. The Heat of Hydration cup is zeroed, and 100 ± 10 grams are added to the cup before placing in the Calimetrix machine at 23°C (ASTM C1702). Heat released by the sample as it hydrates is measured through the use of heat flow sensors in the Isothermal Calorimeter. The sensors are connected to a computer, which records the data for graphing purposes every minute for the first 72 hours. From the data and resulting graphs, the total heat of hydration, initial set, and final set can be estimated (Hu et al. 2014). The calorimeter used in this study is seen below in Figure 3.4.



Figure 3.4. Isothermal Calorimeter

3.5.4. Autogenous Shrinkage

Finally, the autogenous shrinkage test is a which tracks the shrinkage of the sample over the first 72 hours after mixing. After mixing is complete, the mortar is cast into a corrugated tube which is supported by a wood frame and PVC tube which sits on top of a vibration table. The PVC tube is a 1" thin wall and is placed inside of a 1 1/8th in. hole drilled through the piece of wood. The bottom of the corrugated tube is in contact with the vibration table beneath the wood frame, which is physically connected via clamps to the vibration table. Figure 3.5 shows the apparatus with the PVC support tubes.



Figure 3.5. Support Frame for Casting Autogenous Shrinkage Samples

Once the mortar is sealed inside the corrugated tube, the PVC support tube is picked up with the corrugated tube still inside and moved to a controlled environmental chamber where the autogenous shrinkage testing frame is located. Using the reference bar to zero the LVDT's, the sample is then placed in the frame (ASTM C1698). At this point, the autogenous shrinkage program is run via a computer connected to the LVDT's where the LVDT measurement is taken and recorded every 60 seconds. After completion of the test, the data is then adjusted to have Time Zero of the test match the time of final set in the heat of hydration test. The testing frame and LVDT's can be found in Figure 3.6.

Autogenous shrinkage is the very early age shrinkage occurring in cementitious based materials. In early age measurements, hydration has a direct effect on the results of

the test being performed. Because of this, it is critical to understand the mechanisms behind hydration before data analysis. The first step in understanding hydration and autogenous shrinkage is determining when Time Zero (T_0) occurs. T_0 is the time where autogenous shrinkage begins to be measured, however, defining what this point is, is difficult. Due to the varying nature of hydration, choosing an arbitrary point in time is not an option. Initial set is an option for use, but because the mortar can still undergo plastic deformation, this shrinkage data can vary and could be considered not appropriate when attempting to measure the early age shrinkage. This leaves final set as the point which is acceptable for T_0 . Final set is found from the heat of hydration curves as seen above through the first derivative and is used as the starting point for measuring post-plastic deformation (Hu et al. 2014). Measurements of the samples are taken continuously every minute for 72 hours and then graphed and plotted (Zhang et al. 2020). Using 72 hours is related to the Heat of Hydration curve. Because both Heat of Hydration and Autogenous Shrinkage are interconnected, using the same time scale allows both graphs to match each other. Furthermore, a well-prepared sample will not experience much shrinkage after 72 hours compared to what was experienced prior.



a) LVDT's with autogenous shrinkage samples



b) Autogenous shrinkage samples after casting

Figure 3.6. Autogenous shrinkage test apparatus and samples

3.6. Hardened Mortar Tests

3.6.1. Compressive Strength

Hardened mortar casting begins after the fresh mortar tests are complete, which is approximately 12 minutes after beginning to mix. For the compressive strength, three cubes are tested at each of the ages 3 days, 7 days, and 28 days. In accordance with ASTM C109/109M, the loading rate for the compressive strength is between 900 N/s and 1800 N/s (200 and 400 lbs./s) and reasonably held between 1125 and 1575 N/s (ASTM C109/109M). The testing frame used for this is seen in Figure 3.7.



Figure 3.7. Compressive strength apparatus

3.6.2. Drying Shrinkage

For the drying shrinkage bars, the samples are measured after demolding, then submerged in lime saturated water for the next 28 days. After completing the four weeks submerged, the samples are removed and placed in a controlled environmental chamber at 23°C with a relative humidity of 50%. Continuing measurements of the samples are taken at the 4-day, 7- day, 14- day, 28- day, 8- week, 16- week, 32- week, and 64- week dates in accordance with ASTM C596 (ASTM C596).



Figure 3.8. Drying shrinkage testing apparatus

3.6.3. Microstructure Analysis

As part of confirming the increase in the C-S-H generated- as well as the presence of C-A-S-H- in the use of nanomaterials, the use of a Scanning Electron Microscope was employed. In this, the samples were prepared at multiple ages for analysis later. An initial sample was cast, with a smaller sample cut away at the appropriate ages. Smaller samples were placed in acetone in order to prevent further hydration.

After samples were removed from the acetone, they were placed in a mold in order to cast a resin around it. Leaving the resin to cure for 24 hours resulted in a strong enough sample to be cut yet again in order to expose a surface. This exposed surface is coated in gold, which increases the conductivity of the sample, and improves the visual quality of images. Images of the samples can be found below in Figure 3.9 and the diamond tipped saw in Figure 3.10.



Figure 3.9. SEM Samples before and after resin casting



Figure 3.10. Diamond tipped saw

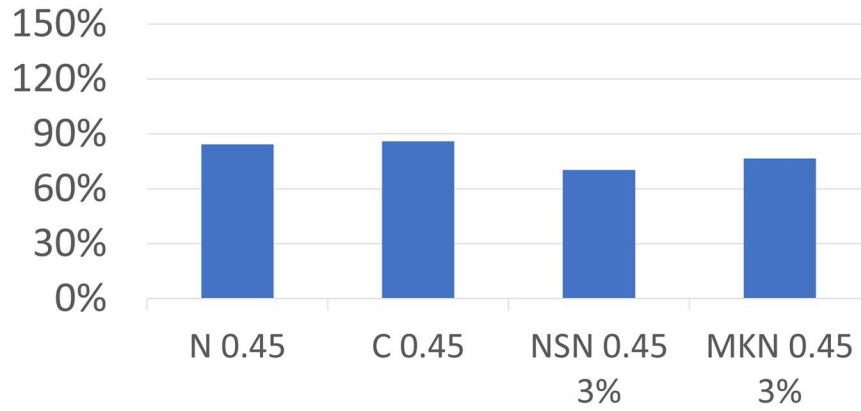
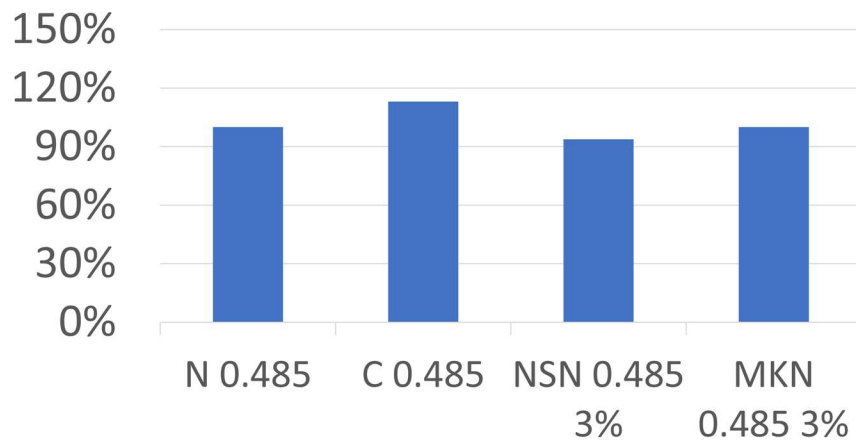
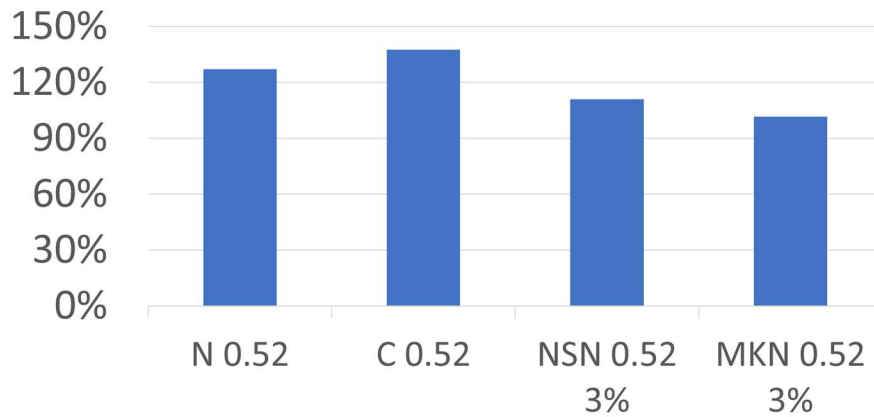
Specimens prepared for this section covered two ages, 1 day and 7 days, in order to see the effects over time. These times were specifically chosen because of the expected change over this period, making the differences between ages stand out more than other choices. When considering the which samples were to be inspected, only two cement types were considered, coarse and Type I/II. From this, only the w/c ratio of 0.485 is chosen. Additionally, both metakaolin and nanosilica samples are chosen for this imaging. The result is 12 samples inspected, six at the age of 1 day and 7 days each.

CHAPTER 4. RESULTS AND DISCUSSION

This chapter is designed to present details of the experimental results from this study. Subsections of this section were based on a general property of mortar, with the relevant properties being workability, heat of hydration, compressive strength, microstructure analysis, and shrinkage.

4.1. Workability

The addition of nanomaterials into concrete and mortar are known to change the properties. In accordance with ASTM C1437 (ASTM C1437), the flow table test results provide an answer to how the metakaolin and nanosilica influence the workability. Additionally, changing the cement type was investigated for changes in workability, with coarse cement providing the expected result of a higher flow value than the Type I/II used as a reference. Including either of metakaolin or nanosilica in the mixes strongly decreased the workability. Increasing the dosage from the initial 3% to 5% caused further reduction to workability and flow reduction. The results for the changing w/c can be found below in Figure 4.1. From the flow table tests, a general trend for both water content and dosage of nanoparticles exists. More flowable mixes are those which use the coarse cement and a higher w/c . Conversely, the mixes with nanoparticles, low w/c , and a finer cement are less flowable due to increased water demand associated with increased fineness.

a) Flow table results of w/c 0.45b) Flow table results of w/c 0.485c) Flow table results of w/c 0.52**Figure 4.1.** Flow table test results with changing w/c

Adding higher dosages of either nanosilica or metakaolin will decrease the flow table results further than the mixtures presented above in Figure 4.1. It is also important to note the higher dosages of nanoparticles will not fully mix with the water during the high shear blending step of the mix procedure. When this occurred, water used in the high shear blending is washed back into the container to remove the remaining nanomaterial. Nanosilica specifically decreased the flow further than the metakaolin, especially at a dosage of 5%. The results to changing the dosage of nanomaterials can be found in Figure 4.2. As stated before, increasing fineness of the materials decreases the overall workability of the material. Increasing the dosage of nanomaterials further exacerbates this property.

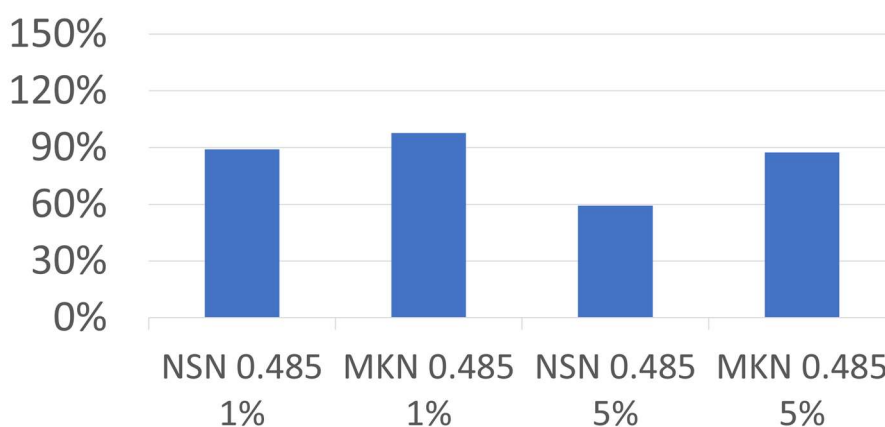


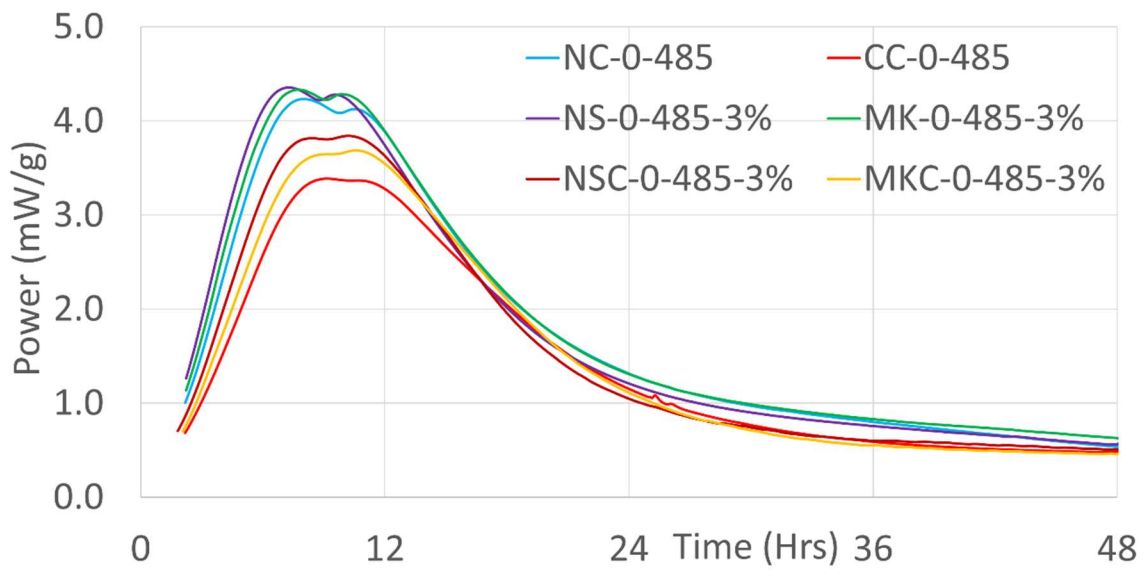
Figure 4.2. Flow table test results of changing dosage of nanoparticles

It is noted from literature, in order to maintain flow from the reference mix design, the mixture with nanomaterials experience an increased water demand (Tobón et al. 2010). Srinivas (2014) attributes the change in workability to a higher packing density when nanoparticles are added. Further work by Sobolev (2006) with nanosilica also found a similar reduction in the flow and workability. For metakaolin, Sabir et al. (2001)

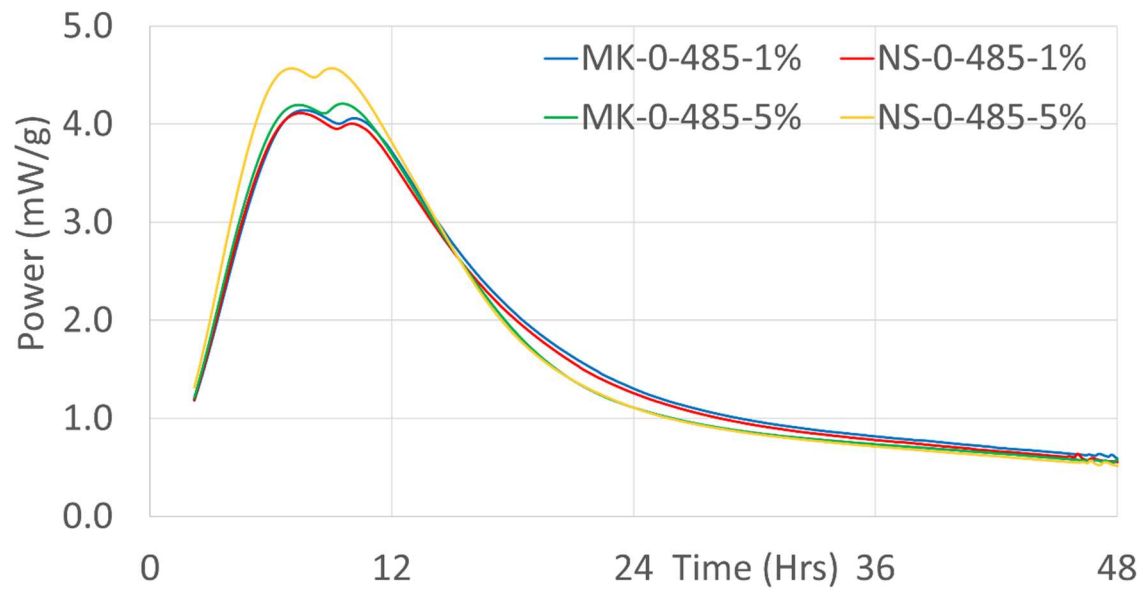
and Siddique and Klaus (2009) both found a similar reduction in the flow table results. Sabir et al. (2001) specifically mentions the reduction of high-range water reducer needed to retain workability in comparison to silica fume, a reduction of around 25-35%. Furthermore, the reduction of workability by the addition of metakaolin is attributed to the filler effect described by Siddique and Klaus (2009).

4.2. Heat of Hydration

Hydration rate and the energy produced during the hydration phase can be correlated through curves. The curve is generated by graphing the recorded data of the first 48 hours of the mix, recording the thermal energy reading at every minute. From this curve, it can be inferred how active the mix design is during hydration. While the complexity of hydration is discussed later, the immediate takeaways from the graphs should be the peaks; specifically, how high the peaks are and where they occur in time found in Figure 4.3. The heat of hydration curves for the mixes of Type I/II cement match very closely to the to the mixes including nanoparticles. Metakaolin and nanosilica both increase the energy generated during hydration.



a) Heat of hydration curve for changing cement fineness with nanoparticles



b) Heat of hydration curve for changing nanoparticle dosage

Figure 4.3. Heat of hydration curves

Noticeably, the first peak for both NSN and MKN occur before the peak of the NC mix. The difference between the two nanoparticles is exposed when increasing the dosage in mixes. At a dosage of 5% with nanosilica, the curve is very pronounced and stand out as opposed to the same dosage of metakaolin, which retains the curve despite

the change in dosage. The difference between these two curves can be attributed to the lower fineness of metakaolin than nanosilica, thus reducing the interactivity from the nucleus effect.

When looking at NC alone, there are two peaks and a higher amount of energy released than CC and its more plateau-like feature. This difference in the graphs is supported by the idea of a coarse cement hydrating more slowly and producing less heat (Liu 2014). In chemistry, the reaction speed of a larger surface area is faster than that of a smaller surface area. Work performed under Holt agrees with the data presented when Holt compared Finnish cements with varying levels of fineness (2001). Sobolev et al. (2006) notes the use of nanoparticles increases the reactivity of the tricalcium silicate (C_3S) in his work as well, again, supporting the results of nanosilica and metakaolin increasing the energy produced in the heat of hydration graphs (Sanchez & Sobolev 2010).

The cause of the increase in energy generated can be attributed to the third effect discussed in this paper, the “Nucleus Effect”. This effect is where the nanoparticles act as additional points of contact where cement can hydrate. By increasing the possible contact points where nucleation can occur, the result is an increase in the energy produced during hydration, which can be seen when the dosage of nanosilica is increased to 5% and below in

Table 4.1.

Table 4.1. Heat produced during isothermal calorimeter testing

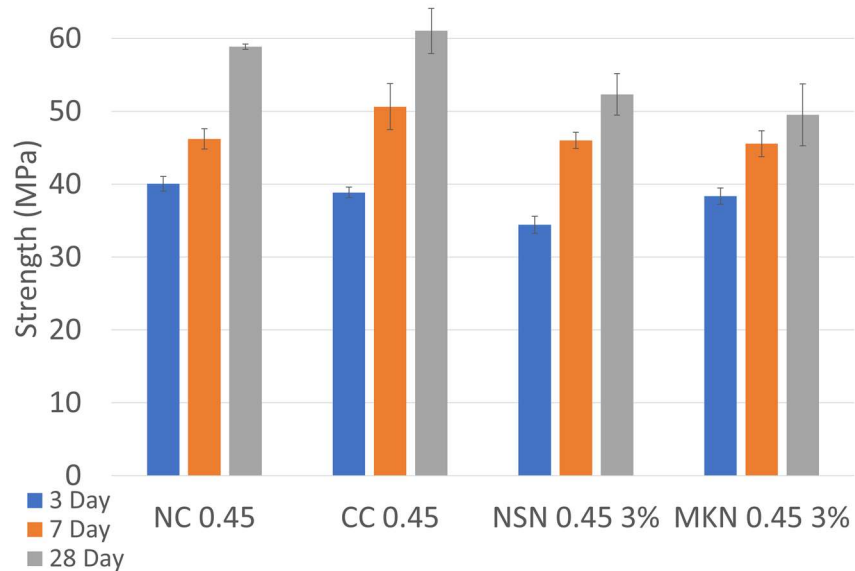
Mixture ID	Total Heat Generated (Millions of Joules)			
	6 Hour	12 Hour	24 Hour	48 Hour
NC-0.485	0.0967	0.812	4.09	13.6
CC-0.485	0.0964	0.599	3.30	11.3
NSN-0.485 3%	0.118	0.939	4.45	14.3
MKN-0.485 3%	0.104	0.852	4.19	13.8
NSC-0.485 3%	0.0084	0.736	3.83	12.5
MKC-0.485 3%	0.0722	0.657	3.58	11.9
NSN-0.485 1%	0.107	0.849	4.09	13.4
MKN-0.485 1%	0.102	0.812	3.95	13.0
NSN-0.485 5%	0.136	1.08	4.99	15.7
MKN-0.485 5%	0.110	0.874	4.17	13.3

In addition to the increase in silica present during hydration from nanosilica, metakaolin also introduces aluminum to the equation. The Pozzolanic Reaction uses the additional silica from the nanoparticles and consumes the calcium hydroxide (C-H) in the cement paste to form calcium silica hydrate (C-S-H). However, with the addition of aluminum, the Pozzolanic Reaction expands to form Calcium Aluminum Silica Hydrate (C-A-S-H) and Calcium Aluminum Hydroxide (C-A-H) in addition to the C-S-H (Sabir et al. 2001). However, the Pozzolanic Reaction does have a limit as it is less active at 10% dosage than at 5% (Siddique & Klaus 2009).

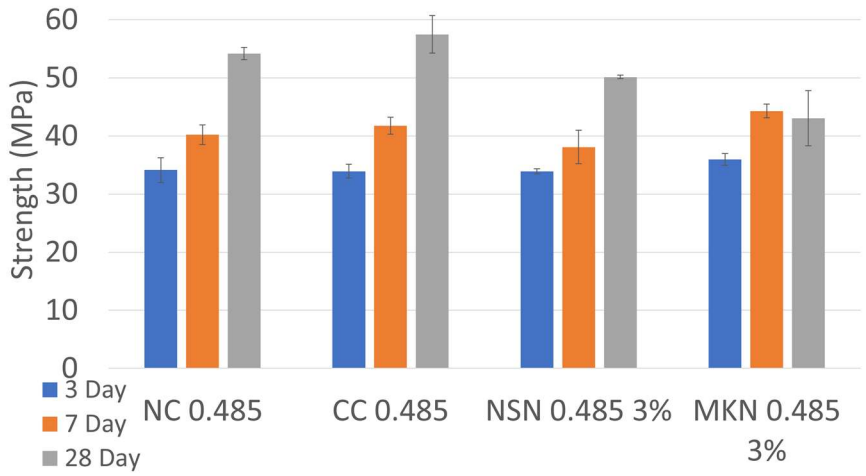
4.3. Compressive Strength

In the compressive strength test, the focus was on the coarse cement and its comparison to Type I/II. From this, changes to the w/c ratio are explored. Finally, changes to dosage as well as changes to cement fineness with nanomaterials is shown.

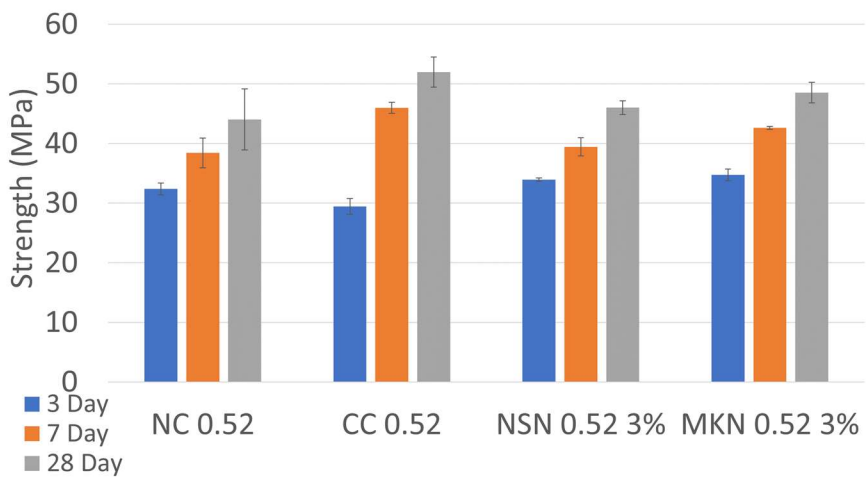
The coarse cement compares well in the compressive strength tests compared to the Type I/II cement despite the expected lower early strength. Mixture designs using the coarse cement outperformed the mixes with Type I/II after the 7-day strength tests across all mixtures. The results for this can be seen in Figure 4.4. Of note, by increasing the w/c , the coarse cement mixes performed increasingly better in comparison to the Type I/II. The gap between the N.C. mixes and C.C. mixes at 28 days increased compared between w/c ratios of 0.45 and 0.52 despite the overall strength reduction (Burrows 2012).



a) w/c 0.45



b) w/c 0.485

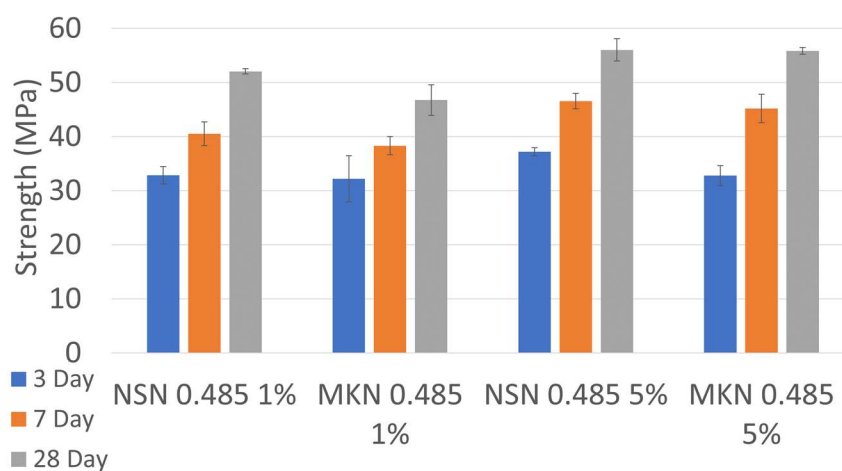


a) w/c 0.52

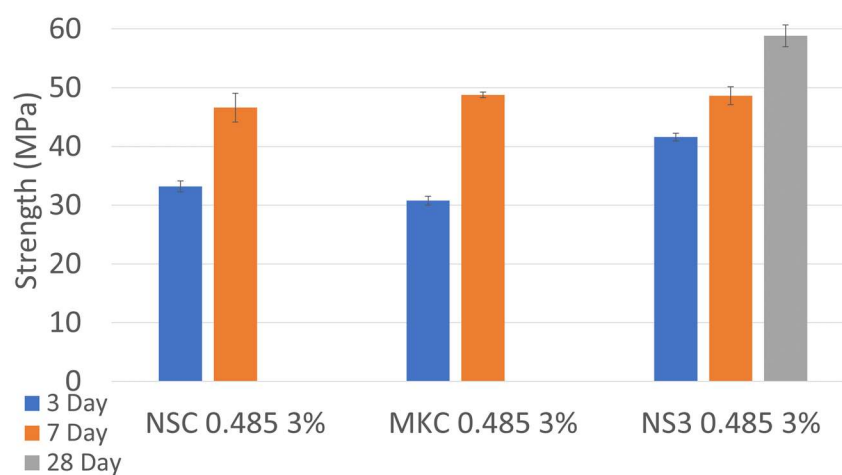
Figure 4.4. Compressive strength results from changing w/c ratio

Using a coarse cement gives the expected result of lower compressive strength at the 3-day mark. Adding in nanomaterials to the coarse cement mixture did increase the 3-day strength, however the larger increase in strength comes at the 7-day mark. The strength of these mixtures is significantly above the compressive strength of the Type I/II alone and the Type I/II with the nanoparticles. Based on the trend of dosages in Figure

4.5, it can be expected that increasing the dosage of the nanomaterial in coarse cement mixtures would further benefit the compressive strength.



a) Changes in nanoparticle dosage



b) Changes in cement fineness

Figure 4.5. Compressive strength of changing dosage and fineness

The addition of nanoparticles into the mortar mixes increased the strength in early ages, specifically 3-day and 7-day. It should be noted, at the 28-day strength tests, the results decreased below the reference; corroborated by work performed by Sobolev et al.

(2006). Sobolev et al. (2006) attributes the increase in strength to the Filler Effect and increased hydration from the pozzolanic reaction (Pozzolanic Effect) resulting in increased C-S-H in the mortar. In agreement with Sobolev is Choolaei et al. (2012) in regard to the filler effect as the method of increasing the strength of mortar with nanoparticles in their work with oil well cement. the reduction of free water is specifically noted. Additionally, Siddique and Klaus (2009) in work with metakaolin pointed toward the decrease in porosity as evidence toward the filler effect.

4.4. Microstructure Analysis

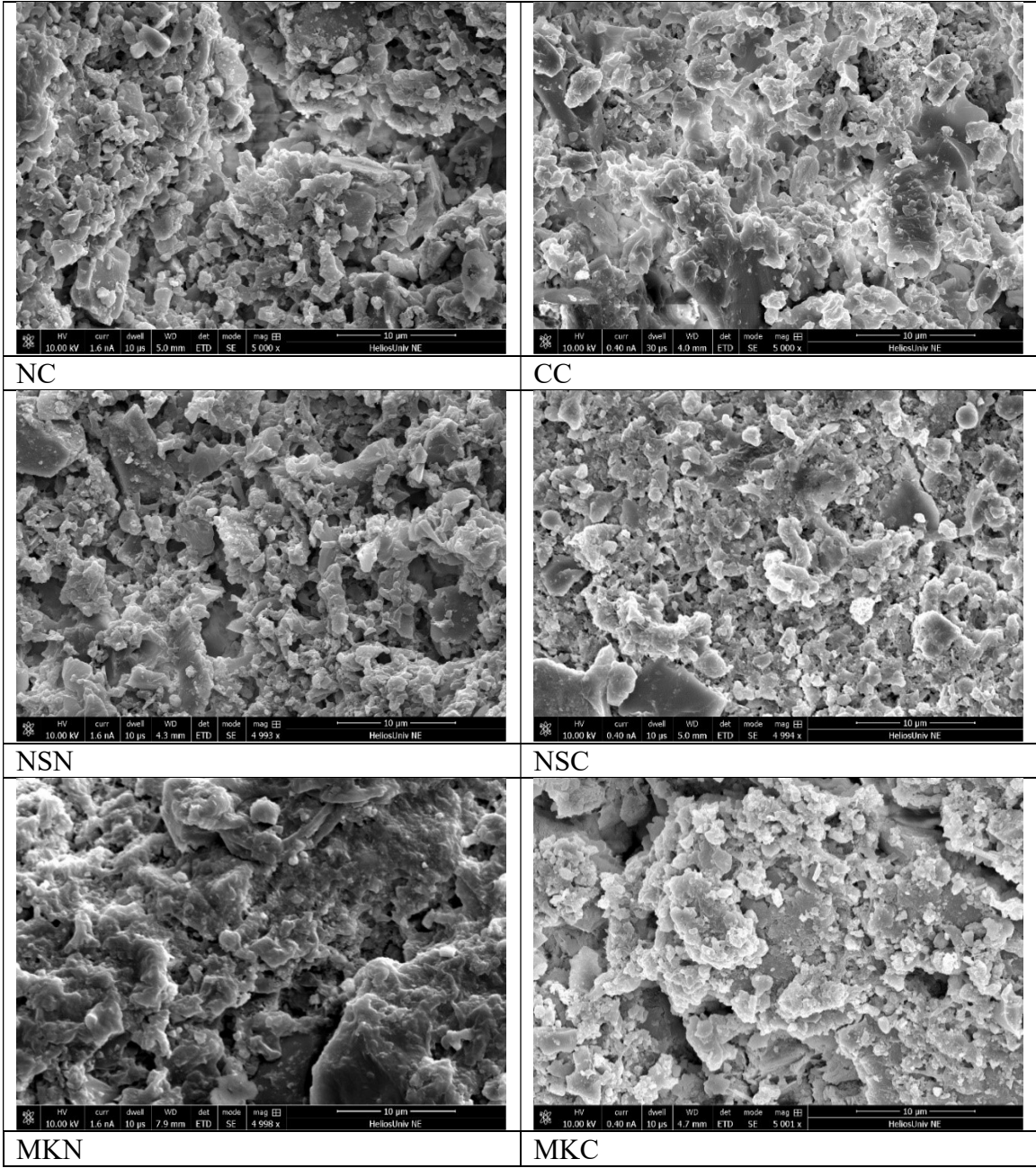
The use of nanomaterial is known to increase the C-S-H gel content of the cementitious matrix. As part of this, there is an increase in the density of the gel as well. Corresponding to this increase in gel content and density, there is an associated increase in compressive strength and flexural strength.

From the images below in Figure 4.6 and Figure 4.7, there are several confirmations made. First, the use of a coarse ground cement generates a lower amount of hydration products than the cement used currently. Based on the associated compressive strength, flow table, and heat of hydration results, this result was expected.

Secondly, the use of nanomaterials increases the density of the gel in a mix using the same cement type. Based upon visual inspection, there is an increase in the gel generated at the cost of C-H and Ettringite when using a nanomaterial. The increase in compressive strength and heat generated during hydration confirms this result.

Thirdly, the use of metakaolin in particular produces the hydration product known as C-A-S-H, a similar product to C-S-H with the benefit of using the aluminum present.

This is the same product present in Roman Concrete, attributed to increasing the durability of the material.



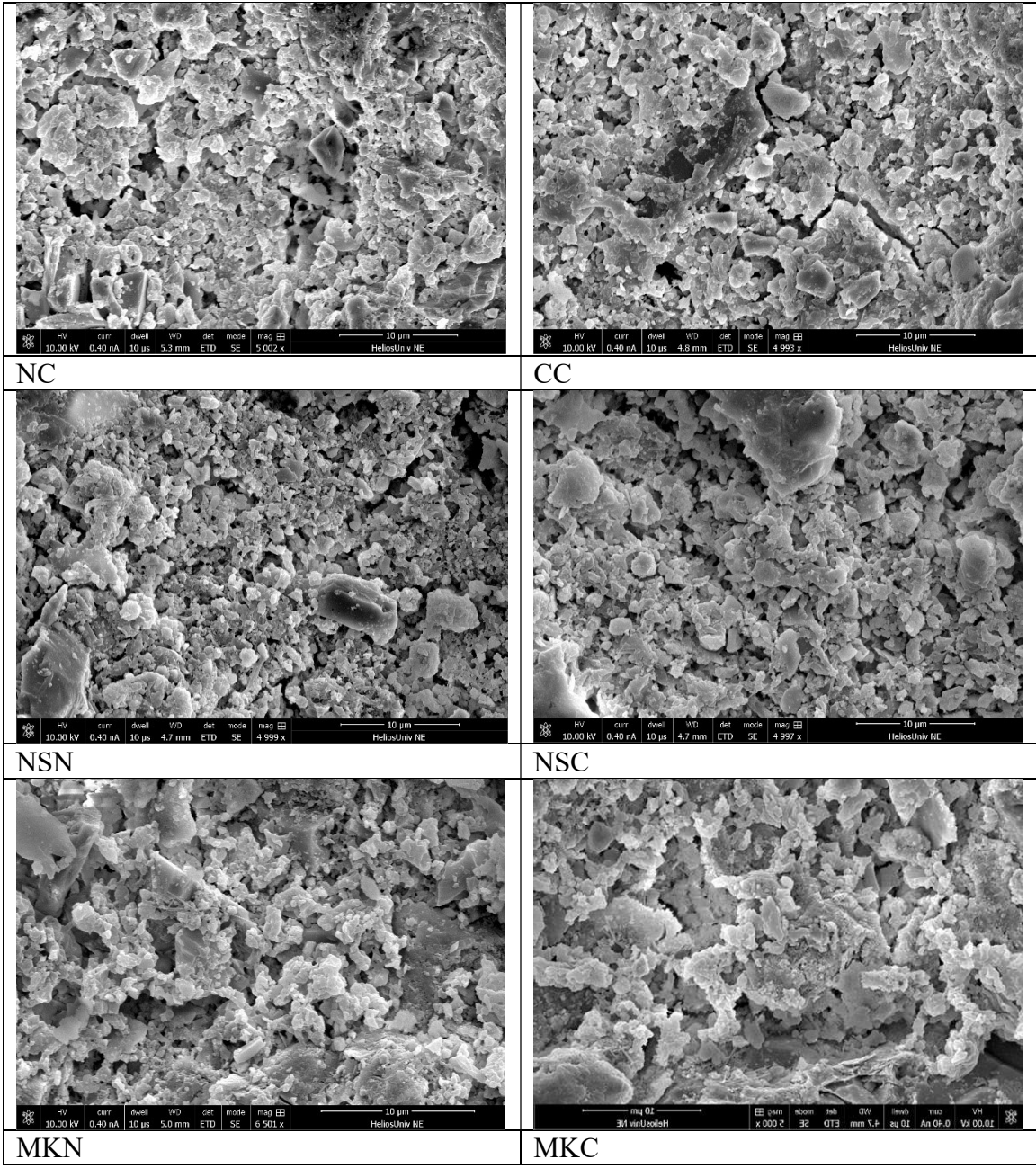


Figure 4.7. SEM images of samples at 7 days of hydration

In the Scanning Electron Microscope (SEM) images, the mixes with coarse cement and nanoparticles show an increase in the C-S-H gel generated at just 1-Day of hydration compared to the gel generated by the NC mix alone at 1-day and even the CC mix at 7-days hydration (Siddique & Klaus 2009). Although the increase in gel generated is not large, it is definitive enough for the MKC and NSC strengths to be nearly identical

to the NC mix at 1-day of hydration. It is important to point out the size and density of the gel created while using the nanoparticles (Glenn 2013). The nanoparticles increased the density of the gel, providing the additional strength seen in the strength results. This increased density can be seen in the SEM images.

During hydration, the cement and water are consumed to produce the products of C-S-H, C-H, and ettringite. The cementitious matrix is composed of 50-70% of C-S-H with the remaining amount a combination of C-H and ettringite (Shah et al. 2008). Diving in deeper to the C-S-H gel, there are two different versions: a high density and low-density gel. Both nanosilica and metakaolin influence the hydration rate and hydration products to produce more high-density C-S-H gel in the cementitious matrix (Gaitero et al. 2010). The high-density gel is the physical reason behind the increase in strength and the lower drying shrinkage. Additionally, the excess amount of silica and aluminum present in a nano and available form, consume the C-H present in the matrix through the Pozzolanic Effect which produce C-S-H and C-A-S-H (Sabir et al. 2001). The Pozzolanic Effect reduces the calcium ions present in the cementitious matrix, reducing a hydration product detrimental to the overall product (Glenn 2013).

4.5. Shrinkage

Hydration is a complicated process with factors such as temperature, particle size, free water availability, and cement content being the largest contributors to the equation. To control these so only particle size influences hydration, environmental temperature is controlled via an isolated chamber and water and cement contents controlled via mixture design. Hydration allows the mortar to gain strength, but it is also the cause of shrinkage in the sample.

Two groups of particles of the same mass and only differing in surface area, will form the same products but at a different speed during a reaction. In short, a larger surface area reacts faster (Liu et. at. 2007). For the mortar in this study, the surface area of the cement is varying and the reaction taking place is hydration. Heat generated during hydration will cause a slight expansion to the material but as the sample cools down, it contracts. This thermal expansion and contraction is the first peak seen in the Figure 4.8. The following peak seen is due to further hydration of the C_3A producing Calcium monosulphate (Holt 2001). As the sample cools down and contracts, free water present is still reacting with the cement. The sample with a higher cementitious surface area reacted more with the free water initially, leading to less expansion during the second expansion phase.

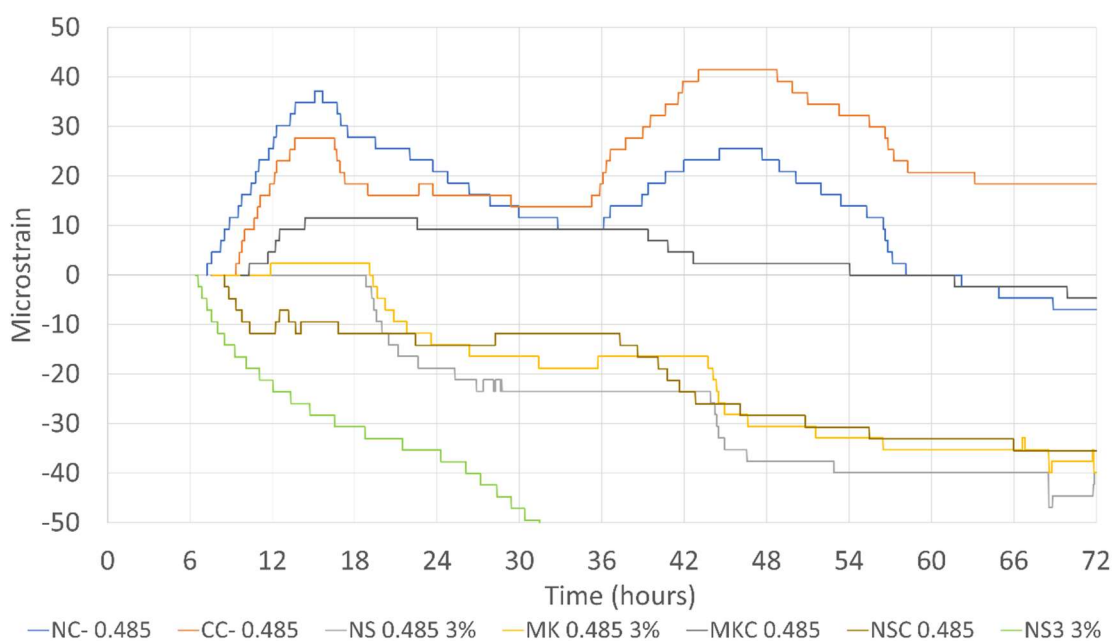


Figure 4.8. Autogenous shrinkage results

During the second shrinkage phase, self-desiccation of the samples due to voids remaining from hydration dominates as the controlling factor. These voids collapse as the void cannot support the tensile stresses developed as pore pressure during the second expansionary phase. A coarse ground cement, with a smaller surface area, reacts more readily with the water later in the hydration process due to less of the cement reacting initially. As a result, there is less pore pressure generated in the initial 24 hours, resulting in less tensile stresses to resolve and less shrinkage (Liu et. at. 2007). Early age changes to length are directly related to the tensile stresses developed. As expected, too high of stresses result in cracking of the sample. It is noted by Fu (2011) and Bentz et al. (2008) that autogenous expansion could occur, however, the expansion is limited to coarse ground cements. Both of these studies support the result above where the coarse cement CC-0.485 resulted in net expansion at the end of 72 hours.

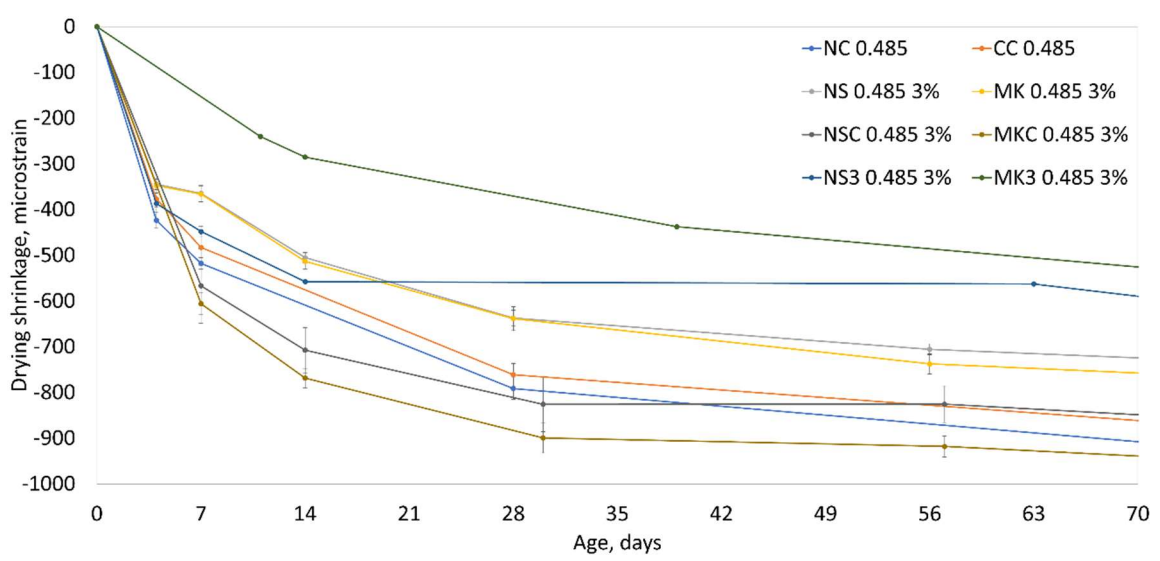
In Figure 4.8, the mixtures with nanoparticles are shown with the N.C. and C.C. Immediately, the conclusion is the use of nanoparticles with Type I/II cement increases the autogenous shrinkage beyond that of the N.C. mix itself. However, because of the Nucleus Effect with nanoparticles, there is almost no expansion seen in the N.S.N. and M.K.N. mixes. When comparing these to the N.S.C. and M.K.C. mixes, the expectation was the autogenous shrinkage would decrease. However, only the metakaolin decreased the shrinkage. This result can be attributed to the lower fineness of metakaolin compared to nanosilica. Using a Type III cement at this point with the nanoparticles resulted in extremely high autogenous shrinkage, up to 100 microstrains at 72 hours. This high degree of shrinkage was expected given the increased fineness of a Type III cement, however, the 100 microstrain result was higher than the predicted 50-70 microstrains.

Nanosilica appears to be the least useful as all mixes showed more shrinkage compared to the mixes with metakaolin. In the mixes with Type III cement, a significantly larger amount of shrinkage occurred, providing strong evidence toward the use of nanoparticles increasing the pore pressure and inducing shrinkage to resolve the pore pressure. Accelerated hydration with nanosilica, as noted by Almohammad & Behfarnia (2020) and Wang et al. (2020), increases the early shrinkage of a sample. However, this work did not work directly with autogenous shrinkage. Wang et al. (2020) points out nanosilica mixes having a very high degree of chemical shrinkage in the first three days of testing, further supporting the first 72 hours as the key timeframe. Gleize et al. (2007) also found a high degree of autogenous shrinkage in mixes with metakaolin, and also the plateau (decrease in the change in length) experienced by samples after the 72-hour mark.

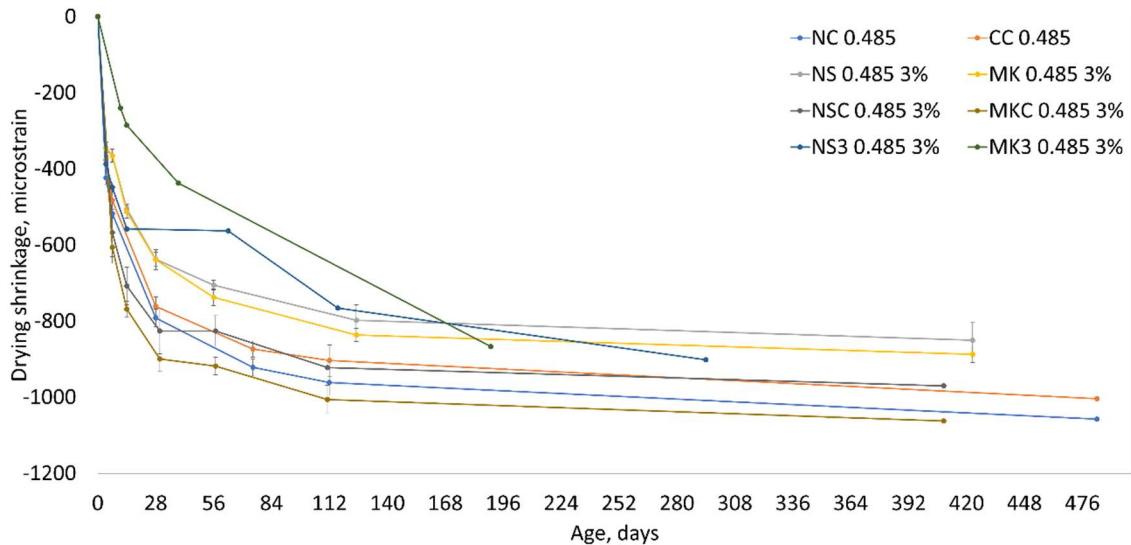
Mixtures using nanoparticles show a distinct contraction during the first 72-hours. The process behind this comes from the same mechanism driving the increased thermal energy in the Heat of Hydration test; the additional points of nucleation from the nanoparticles increase the rate of hydration and the pore pressure (tensile stresses) generated via hydration (Bentz et al. 2008). Resolving the tensile stresses causes the high degree of shrinkage seen in the samples.

Moving to drying shrinkage, the results can be found in Figure 4.9. From the initial glance, C.C. performs better (less shrinkage) than the N.C. mixture. This was to be expected given the slower hydration reaction for the C.C. mixture and thus lower tensile stresses developed which need resolving. Mixtures using the nanoparticles depart from the expected trend. The N.S.N. and M.K.N. mixtures outperform the C.C. mix by 10%

roughly, or approximately 100 microstrains at an age of 70 days. While the expected trend would be for coarse cement mixtures to outperform the Type I/II, this is not true for the N.S.C. and M.K.C., as these mixtures performed worse than N.C. The explanation for this unexpected result is due to the stresses generated during hydration being lower and not being resolved in the autogenous shrinkage.



a) Mid-term drying shrinkage



a) Long-term drying shrinkage

Figure 4.9. Long- and mid-term drying shrinkage

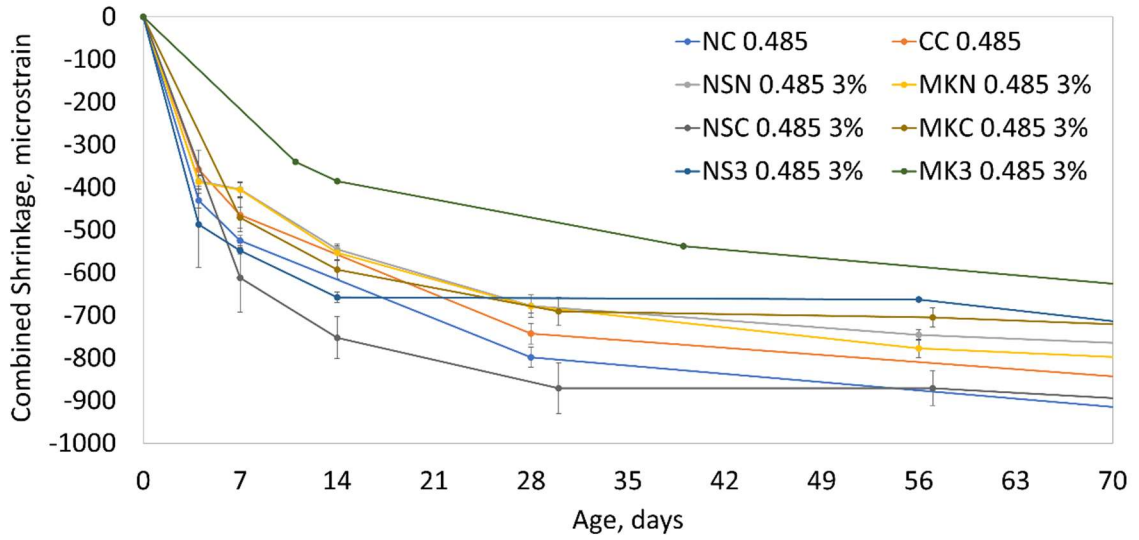
In work with nanosilica, Birgisson et al. noted a reduction in shrinkage when using nanosilica, attributing the reduced shrinkage to the densification of the cement matrix. Metakaolin also reduces the long-term shrinkage of the material, however, early age shrinkage does increase (2012).

Finally, for a fair comparison between mixes, combining the drying shrinkage graph and autogenous shrinkage graph is completed. The microstrain value at the 72 hours for the autogenous shrinkage is added to the results of the drying shrinkage. The cross-sectional area of the samples is close enough to be considered equal. In addition, the two samples are at a different age. For the drying shrinkage test, the procedure calls for samples to be cured for 28 days. In doing this, the cementitious matrix is already developed by the time testing begins and will not take into account the high tensile

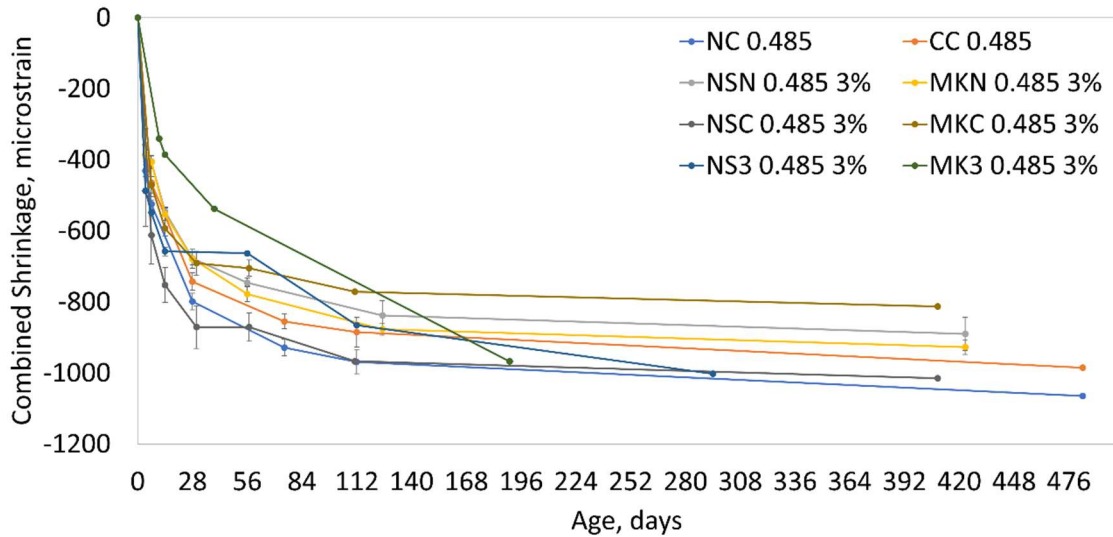
stresses being resolved. In order to account for the shrinkage occurring when the cementitious matrix is weak, the autogenous shrinkage for the same mixture is added to the drying shrinkage test results. Autogenous shrinkage results are the direct representation of the resolving of tensile stresses and are not long term. In adding these together, the combined shrinkage will better reflect the shrinkage a sample undergoes as the addition of the first 72 hours of shrinkage are known and expressed in the same numerical form as the drying shrinkage test.

Through doing combined shrinkage, a pseudo-worst-case scenario is produced and a comparable platform across all mixes is created. Upon examining the results of the combined shrinkage, M.K.N. and N.S.N. are the clear beneficiaries seen in Figure 4.10. However, M.K.C. and N.S.3. are also on a similar track of lower shrinkage than both C.C. and N.C. The Type III cement was used here to provide an additional point of fineness for comparison after the initial results of the drying shrinkage.

Looking at the long-term data though, mixtures with Type III cement continue to shrink despite what appeared to be a plateau in the mid-term figure. The coarse cement with metakaolin mixture continues to perform well, with a very long plateau before 800 microstrains, a 20% benefit over the Type I/II after 420 days. N.S.C disappoints again, as the expectation would be more similar to M.K.C. This however, can be yet again returned to nanosilica having a significantly higher fineness than metakaolin, resulting in higher pore pressures despite the benefits of using a coarse cement in reducing pore pressure and tensile stresses.



a) Mid-term combined shrinkage



b) Long-term combined shrinkage

Figure 4.10. Combined shrinkage results

CHAPTER 5. CONCLUSION AND RECOMMENDATIONS

5.1. Conclusions

Through a comprehensive experimental study of the performance of concrete with different cement fineness and nan-activators, the following conclusions can be made:

- Coarse ground cements are beneficial in reducing the shrinkage of concrete, both autogenous shrinkage and drying shrinkage.
- The increase in strength when using nanoparticles is sufficient and outpaces the strength gain of current concrete. This also applies to mixtures which use a coarse cement with the nanoparticles.
- Comparing mixtures based on combined shrinkage is more beneficial than only comparing from drying shrinkage. Drying shrinkage does not account for the resolving of tensile stresses because of the excess water involved in the procedure. The tensile stresses from pore pressure must be accounted for when comparing concretes. The difference can be directly seen in the mixture M.K.C.
- Using nanoparticles increases the pore pressure generated during the hydration process due to the nucleation effect. This pressure is released early during the autogenous shrinkage phase when the concrete is weaker. Due to the filler effect and pozzolanic effect, the pores in the cementitious matrix are smaller and the matrix overall is strengthened. Between these forces, the result is shrinkage is resolved sooner through the autogenous shrinkage and drying shrinkage is reduced.

- The increased generation of C-S-H, as well as the presence of C-A-S-H for metakaolin, promotes a stronger cementitious matrix resulting in increased strength and decreased drying shrinkage of the mixture.

5.2. Recommendations for Future Work

- Coarse cement shows a clear benefit over the Type I/II used currently in the industry. With this in mind, finding a break-even point where Blaine is still lower than modern cement, yet is able to significantly reduce shrinkage but can still reasonably reach strength of the contractor needs would be ideal. This would remove the need to use any nanomaterials.
- Currently, the method of introducing the nanomaterials into concrete is via water. While this does allow for good dispersion, blending with the cement prior to mixing should also be investigated. Creating a nano-activated coarse cement would then be similar to other blended cements such as Type I.P. or Type I.L.
- This study focuses primarily on metakaolin and nanosilica despite other options being available. Replicating these tests with nanotitanium to take advantage of nanotitanium's photocatalytic effect should be encouraged. Any additional benefits to the concrete beyond what was found in this study should be welcomed.
- In addition to the previous point, study of the effects of using nanosilica and nanotitanium together in a blend could be beneficial. The benefit of additional silica in the cementitious matrix and the self-cleaning ability of titanium would provide a very durable concrete.

- Perform a full cost analysis of the concrete with nanomaterials and coarse cement.

The cost savings of a coarse cement, plus the longevity of the new concrete can provide a much more cost efficient material than the concrete currently used.

REFERENCE LIST

- Akpan, U. G., & Hameed, B. H. (2010). The advancements in sol–gel method of doped-TiO₂ photocatalysts. *Applied Catalysis A: General*, 375(1), 1-11.
- Almohammad-albakkar, M., & Behfarnia, K. (2020). Effects of the combined usage of micro and nano-silica on the drying shrinkage and compressive strength of the self-compacting concrete. *Journal of Sustainable Cement-Based Materials*, 1-19.
- ASTM International. *C39/C39M-21 Standard Test Method for Compressive Strength of Cylindrical Concrete Specimens*. West Conshohocken, PA; ASTM International, 2021.
- ASTM International. *C109/C109M-20b Standard Test Method for Compressive Strength of Hydraulic Cement Mortars (Using 2-in. or [50 mm] Cube Specimens)*. West Conshohocken, PA; ASTM International, 2020.
- ASTM International. *C128-15 Standard Test Method for Relative Density (Specific Gravity) and Absorption of Fine Aggregate*. West Conshohocken, PA; ASTM International, 2015.
- ASTM International. *C150-21 Standard Specification for Portland Cement*. West Conshohocken, PA; ASTM International, 2021.
- ASTM International. *C230/C230M-21 Standard Specification for Flow Table for Use in Tests of Hydraulic Cement*. West Conshohocken, PA; ASTM International, 2021.
- ASTM International. *C305-20 Standard Practice for Mechanical Mixing of Hydraulic Cement Pastes and Mortars of Plastic Consistency*. West Conshohocken, PA; ASTM International, 2020.
- ASTM International. *C596-18 Standard Test Method for Drying Shrinkage of Mortar Containing Hydraulic Cement*. West Conshohocken, PA; ASTM International, 2018.
- ASTM International. *C1437-20 Standard Test Method for Flow of Hydraulic Cement Mortar*. West Conshohocken, PA; ASTM International, 2020.
- ASTM International. *C1698-19 Standard Test Method for Autogenous Strain of Cement Paste and Mortar*. West Conshohocken, PA; ASTM International, 2019.
- ASTM International. *C1702-17 Standard Test Method for Measurement of Heat of Hydration of Hydraulic Cementitious Materials Using Isothermal Conduction Calorimetry*. West Conshohocken, PA; ASTM International, 2017.
- Bentz, D. P., Sant, G., & Weiss, J. (2008). Early-age properties of cement-based materials. I: Influence of cement fineness. *Journal of materials in civil engineering*, 20(7), 502-508.

- Birgisson, B., Mukhopadhyay, A. K., Geary, G., Khan, M., & Sobolev, K. (2012). Nanotechnology in concrete materials: A synopsis. *Transportation research circular*, (E-C170).
- Brooks, J. J., & Johari, M. M. (2001). Effect of metakaolin on creep and shrinkage of concrete. *Cement and concrete composites*, 23(6), 495-502.
- Burrows, R. (2012, November 15). *Concrete Durability: Is American Portland Cement Inferior to European Cement*. Concrete Construction. https://www.concreteconstruction.net/how-to/materials/concrete-durability_o.
- Burrows, R. (2007, January 24). *The Life and Death of Type II Cement*. Concrete Construction. https://www.concreteconstruction.net/how-to/construction/the-life-and-death-of-type-ii-cement_o.
- Choolaei, M., Rashidi, A. M., Ardjmand, M., Yadegari, A., & Soltanian, H. (2012). The effect of nanosilica on the physical properties of oil well cement. *Materials Science and Engineering: A*, 538, 288-294.
- Courard, L., Darimont, A., Schouterden, M., Ferauche, F., Willem, x., & Degeimbre, R. (2003). Durability of mortars modified with metakaolin. *Cement and Concrete Research*, 33(9), 1473-1479.
- Fu, T. (2011). Autogenous deformation and chemical shrinkage of high performance cementitious systems.
- Gaitero, J. J., Campillo, I., Mondal, P., & Shah, S. P. (2010). Small changes can make a great difference. *Transportation Research Record*, 2141(1), 1-5.
- Glavind, M. (2009). Sustainability of cement, concrete and cement replacement materials in construction. In *Sustainability of construction materials* (pp. 120-147). Woodhead Publishing.
- Gleize, P. J., Cyr, M., & Escadeillas, G. (2007). Effects of metakaolin on autogenous shrinkage of cement pastes. *Cement and Concrete Composites*, 29(2), 80-87.
- Glenn, J. (2013). *Nanotechnology in concrete: Critical review and statistical analysis*. Florida Atlantic University.
- Gruber, K. A., Ramlochan, T., Boddy, A., Hooton, R. D., & Thomas, M. D. A. (2001). Increasing concrete durability with high-reactivity metakaolin. *Cement and concrete composites*, 23(6), 479-484.
- Holt, E. E. (2001). *Early age autogenous shrinkage of concrete* (Vol. 446). Espoo, Finland: Technical Research Centre of Finland.

- Hu, J., Ge, Z., & Wang, K. (2014). Influence of cement fineness and water-to-cement ratio on mortar early-age heat of hydration and set times. *Construction and building materials*, 50, 657-663.
- Liu, F. (2014). Early-age hydration studies of Portland cement.
- Liu, R., Zhang, Z., Zhong, R., Chen, x., & Li, J. (2007). Nanotechnology synthesis study: research report. *Texas Department of Transportation*.
- Raki, L., Beaudoin, J., Alizadeh, R., Makar, J., & Sato, T. (2010). Cement and concrete nanoscience and nanotechnology. *Materials*, 3(2), 918-942.
- Sabir, B. B., Wild, S., & Bai, J. (2001). Metakaolin and calcined clays as pozzolans for concrete: a review. *Cement and concrete composites*, 23(6), 441-454.
- Sanchez, F., & Sobolev, K. (2010). Nanotechnology in concrete—a review. *Construction and building materials*, 24(11), 2060-2071.
- Schindler, A. K., & Frank McCullough, B. (2002). Importance of concrete temperature control during concrete pavement construction in hot weather conditions. *Transportation Research Record*, 1813(1), 3-10.
- Scrivener, K. L., & Nonat, A. (2011). Hydration of cementitious materials, present and future. *Cement and concrete research*, 41(7), 651-665.
- Shah, S. P., Mondal, P., Ferron, R. P., Tregger, N., & Sun, Z. (2008). News on nanotechnology.
- Siddique, R., & Klaus, J. (2009). Influence of metakaolin on the properties of mortar and concrete: A review. *Applied Clay Science*, 43(3-4), 392-400.
- Silvestre, J., Silvestre, N., & De Brito, J. (2016). Review on concrete nanotechnology. *European Journal of Environmental and Civil Engineering*, 20(4), 455-485.
- Sobolev, K., Flores, I., Hermosillo, R., & Torres-Martínez, L. M. (2006). Nanomaterials and nanotechnology for high-performance cement composites. *Proceedings of ACI session on nanotechnology of concrete: recent developments and future perspectives*, 91-118.
- Srinivas, K. (2014). Nanomaterials for concrete technology. *International Journal of Civil, Structural, Environmental and Infrastructure Engineering Research and Development (IJCSEIERD)*, 1(4), 79-90.
- Tobón, J. I., Restrepo, O. J., & Payá, J. (2010). Comparative analysis of performance of Portland cement blended with nanosilica and silica fume. *Dyna*, 77(163), 37-46.

- Wang, J., Cheng, Y., Yuan, L., xu, D., Du, P., Hou, P., ... & Wang, Y. (2020). Effect of nano-silica on chemical and volume shrinkage of cement-based composites. *Construction and Building Materials*, 247, 118529.
- Zhang, G. Z., Cho, H. K., & Wang, x. Y. (2020). Effect of nano-silica on the autogenous shrinkage, strength, and hydration heat of ultra-high strength concrete. *Applied Sciences*, 10(15), 5202.